Spring 2022

AN EXAMINATION OF THE IMPACTS OF BEAVER DAM MIMICRY STRUCTURES ON GROUNDWATER SURFACE-WATER INTERACTIONS IN LOWER MOUNTAIN RIPARIAN SYSTEMS

Mercedes D. Salazar

AN EXAMINATION OF THE IMPACTS OF BEAVER DAM MIMICRY STRUCTURES ON GROUNDWATER SURFACE-WATER INTERACTIONS IN LOWER MOUNTAIN RIPARIAN SYSTEMS

by

Mercedes D. Salazar

A thesis submitted in partial fulfillment of the
requirements for the degree of

Master of Science in Geology with an Emphasis in Hydrogeology
and a Certificate in Ecological Restoration

Montana Tech

2022

Abstract

Beaver dam analogs (BDAs) are a low cost, low disturbance stream restoration technique that may improve surface-water/groundwater interactions and wetland connectivity. BDAs are intended to imitate the effects of natural beaver dams by slowing stream velocity, promoting infiltration, increasing dry-season streamflow, aggrading the streambed, and capturing organic matter and other nutrients. This study was conducted to evaluate the degree to which these objectives were being met at a study site on Perkins Gulch, southwest Montana, USA.

The Perkins Gulch study area can be summarized by four gauging sites that separate three reaches along the creek. By detailing background processes and separating the field site into reaches with distinct properties, we can understand the temporal and spatial similarities and differences between intact BDAs, blown out BDAs, and abandoned beaver dams. This approach also allows for evaluation of how riparian conditions in these restored reaches compare to historical conditions.

BDAs resulted in increased stream sinuosity and wetland connectivity. Despite recent restoration and observations of continuous annual flow in 2019, several sections of Perkins Gulch ran dry in the 2021 field season. This was caused by anomalously dry conditions, geologic features, and blowout of several BDA structures. An abandoned beaver complex at the site served as a proxy to gauge how BDAs might impact surface groundwater conditions. If BDA structures are repaired and replaced as needed, they may increase local surface/groundwater interactions, provide for continuous streamflow, and alter stream corridor geomorphology.

Keywords: Beaver Dam Analog, wetland connectivity, riparian restoration, stream restoration

Dedication

I would like to dedicate this thesis to the people who knew I could do it, even when I didn't. I cannot begin to thank you enough, but hopefully this dedication is a good start.

This Master's thesis would not have been possible without my family and loved ones. I want to thank my mom for making me a book worm, my dad for making me a scientist, my sister for making sure my writing is up to snuff, and Chase, who has always been there for me, even when 700 miles away. A special thank you goes to my lizard who monitored my work the entire time.

"The scariest moment is always just before you start. After that, things can only get better."

— Stephen King, On Writing: A Memoir of the Craft

Acknowledgements

Advisor:

Dr. Glenn Shaw, Department of Geological Engineering, Montana Technological University

Committee Members:

Andrew Bobst, Montana Bureau of Mines and Geology

Dr. Robert Pal, Department of Biological Sciences

Amy Chadwick, Ecologist at Great West Engineering

Great West Engineering

The Montana Water Center

Table of Contents

List of Figures

1. Introduction

1.1. Global Impact/Study Motivation

In semi-arid settings common objectives of BDA treatments include increasing the storage of water in the stream corridor and increasing dry-season stream flows. Warmer climate conditions and changing population distribution have resulted in both increased water scarcity and reduced ecological health in arid and semi-arid regions globally. "Water demand is projected to increase by 55% globally between 2000 and 2050," (Leflaive, 2012). The number of people living in river basins under severe water stress is projected to reach 3.9 billion by 2050, totaling over 40% of the world's population. In addition, groundwater depletion, which more than doubled between 1960 and 2000, may become the greatest threat to agriculture and urban water supplies in several regions in the coming decades (Leflaive, 2012). In 2015 the United States diverted significantly more surface water than groundwater for anthropogenic use. However, almost all self-supplied domestic water and over 40% of water used for agriculture was groundwater (Water Science School, 2018). In water-stressed basins small changes in water regimes such as droughts can increase competition between human and natural systems, resulting in ecosystem degradation.

More than one third of the Earth's land surface is classified as arid or semi-arid. Reports from the Intergovernmental Panel on Climate Change (IPCC) reports since 1990 have documented global average temperature increases of about 0.2 ℃ per decade. Global climate change has exacerbated climate extremes such that in arid to semi-arid regions there will likely be fewer precipitation events, individual events will be less intense, and there will be more prolonged periods between events (Houghton, 2017).

Ecological restoration primarily aims to restore degraded or destroyed ecosystems to a self-sustaining state. Low-disturbance restoration methods can often be beneficial for both ecosystems

and humans. Low-disturbance restoration often attempts to mimic processes that occur naturally and require little to no additional input after installation. For example, the North American beaver (*Castor canadensis*) is both a keystone species and an ecological engineer that has served as a source of inspiration in using BDAs for riparian restoration.

1.2. Local Impact

Natural beaver dams are constructed of large woody vegetation packed continuously with mud, rocks, and smaller shrubbery. Beaver dams may slow stream velocity, decrease erosion, promote infiltration, raise the local water table, increase dry-season streamflow, and create ecosystem complexity (Castro, 2017; Puttock et al., 2017). Beaver dam analogs (BDAs) mimic natural beaver dams in both form and function and are an effective, cost-efficient method of restoring and creating riparian environments. They are most utilized in small streams and are constructed with natural materials that often originate from the site. BDAs alter in-stream habitats in four key ways: they increase both stream depth and width, create opportunities for flow heterogeneity, increase sediment deposition, and lower average stream velocity (Smith et al., 2013).

The lifecycle of natural and analog beaver dam structures is nonlinear. Typically, young stream systems start as high energy, high gradient systems with low to moderate flow volume. In systems with sufficient flow and appropriately deep and wide channels, a beaver may attempt to build one or two dam structures to slow stream velocity and create ponds. In many cases stream velocity is too great for fledgling beaver dams and after ponding reaches the strength threshold of the dam the structure will fail (aka. blow out). Successful dams can lead to new channelization parallel to the primary stream channel. After a time, increased habitat heterogeneity and raised

water tables can lead to diverse and complex stream and riparian ecosystems, and the development of low energy wetlands. Natural systems like this consist of features like oxbow lakes, point bars, cut banks, floodplains, and braided channels (Butler et al, 2005; Castro, 2017). Each of these features create critical differentiation in both flow velocity and depth (Howard & Larson, 1985; Pollock et al, 2014) leading to dense vegetation and water and nutrient cycling. As such, continued development of the restored wetland may result in increased biodiversity and ecosystem resilience (Bouwes et al., 2016; Castro, 2017; Mitchell & Niering, 1993; Pollock, 2014). For example, both diversity and abundance of fish populations are positively related to habitat heterogeneity. Faster stream flows and coarse substratum downstream of BDA structures increase the array of fluvial habitats available. These changes can be critical for the propagation of fish, whose life cycles depend on slow water to spawn, fast water to grow, and hard substrata which trap small sediments and improve water quality (Davee et al., 2019; Bouwes et al., 2016).

As a beaver dam ages and is strengthened with the addition of biomaterial, increasingly more sediment is stored, driving the streambed to aggrade (Scamardo et al., 2020). Increasing pressure to the top of the dam eventually causes weakening and blowout (Butler & Malansen, 2005; Westbrook et al, 2006: Westbrook et al, 2015). Dam blowouts are high energy and high-volume events that can lead to damaging rises in erosion and can increase sediment load of the stream, albeit briefly (Butler et al., 2005). Temporarily heightened erosion rates can cause the cross-sectional area of the channel to rapidly increase. However, most of the sediment that was stored by the dam over its lifespan remains in-situ during the flood. As a result, the total volume of sediment released by the watershed over time is lower in dammed streams. After initial flooding ends, flow volume returns to natural background levels (Puttock, 2017; Westbrook et al., 2013).

Depending on the physical height and strength of the dam, volume of stream flow, and elevation of the stream banks, a dam structure could create a locally or regionally significant pond. Assuming the dam structure can withstand the water pressure of the pond, the surrounding catchment area increases proportionally with pond area and volume (Butler et al, 2005). One study from New York State examined the impact of BDAs on ponding area, capture area, and discharge area. Post BDA models showed a 30% increase in the surface area of the capture zone. Likewise, the area of the discharge zone increased by over 80%. Over the study period, the surface area of the pond nearly doubled after the installation of a BDA (Feiner et al, 2015).

BDAs similarly alter local groundwater response. Depending on the hydraulic conductivity of the surrounding sediment, subsurface flow velocity can be up to several meters per day (Westbrook, 2006). As such, infiltration rates may exceed average discharge of groundwater causing water table elevation to rise (Puttock, 2017). One study showed that groundwater discharge from wetland ponds increased by 90% after the installation of a BDA (Fiener et al., 2015).

Changes in groundwater elevation due to beaver dams or BDAs are not geologically permanent. For example, after the installation of a BDA in the upper Colorado River area, observation wells in the area gained roughly 10 cm head compared to background levels. After a particularly intense seasonal storm in late July of 2005, the BDA failed. In the following 14 hours the groundwater elevation declined approximately 8 cm. In sediments with moderate hydraulic conductivity, residence time of ground water as well as ground water storage is highly dependent on surface conditions such as the continued existence of a beaver dam (Westbrook, 2006).

Unlike the immediate response of surface and groundwater systems to BDA installation, other benefits such as the growth of woody vegetation and establishment of new channels is a multi-decadal process. Increased channelization and overbank flow of an original stream can raise

the water table and improve the ability for shallow rooting vegetation such as shrubs and grass to propagate (Mitchell et al., 1993; Silverman et al, 2019). According to Mitchell et al. (1993), the average increase of vegetation productivity after the installation of a BDA was over 20% over a five-year monitoring program. A segment of the study, which spanned over 20 years, similarly found an increase in vegetation biomass of over 50% compared to pre-BDA conditions. In this study, beaver dam restoration not only increased overall vegetation productivity but also extended this heightened productivity well into the growing season. Likewise, variation in water availability and vegetation promote populations of large wildlife (Nummi, 1989; Smith, & Mather, 2013).

On average, the largest increases in both vegetation productivity and productive mesic area occur within the first decade after restoration in summer and fall months when rainfall and snowmelt is high (Lautz et al., 2019). During this time, elevation of the water table is at its highest. Because of this, in later months, when snowmelt and rainfall decline a BDA restored stream may be a losing system but will retain some flow as it is fed by groundwater. In both local and regional beaver mimicry study sites, not only are both surface and groundwater being made more available for vegetation growth, but it is likewise being made available for longer periods. Extensions in water availability can have significant benefits to ecosystem function (Naiman et al, 1986).

1.3. Research Goals

Reduced snowpack and increased runoff in high elevation arid and semiarid regions, such as in western Montana, have become critically concerning from both agricultural and conservation perspectives. As such, private and public sectors have utilized low impact restoration methods such as BDAs with the primary goal of storing groundwater during snowmelt and later releasing that water in the dry season to enhance baseflow. In Perkins Gulch, which spans both private and public land, BDAs have been used to improve year-round water availability and to improve riparian health.

This study investigates how BDAs (intact & blown out) and abandoned beaver structures in Perkins Gulch affect groundwater (GW) and surface water (SW) interactions. The impact of BDAs is linked to both spatial and temporal background processes such as geologic setting and seasonal variation (Pilliod et al., 2018). As such, this study focuses on two main questions.

1. How do spatial and temporal processes control surface/groundwater interactions?

2. Given specific geologic setting, how do BDAs alter local hydrology?

By detailing background processes and separating the field site into unique reaches with distinct properties we can understand how intact/blown out BDAs/ abandoned beaver dams are similar and how they differ temporally and spatially as well as how these structures cause deviation from historical riparian background conditions.

2. Site Description

2.1. Monitoring Sites

The Perkins Gulch study area includes 6.5 km of stream, fed by a catchment area of 23.8 km^2. This includes private and public land. The elevation of the monitored reach ranges from 1,465 m to 1,755 m, with a maximum basin elevation of 2,200 m.

Perkins Gulch is east of Warm Springs, Montana and is one tributary to the Clark Fork River. Historical climate data such as precipitation and daily temperature was collected from USDA Warm Springs SNOTEL site 850. This site is at an elevation of 2400 m and thus was assumed to be comparable to the upper area of the Perkins Gulch basin. The average daily precipitation at the Warm Springs monitoring station is 2.72 mm. From 2015 to 2022 the lowest recorded temperature at the Warm Springs was -23.3 ℃, the high was 20.2 ℃, and the daily average was 2.04 ℃.

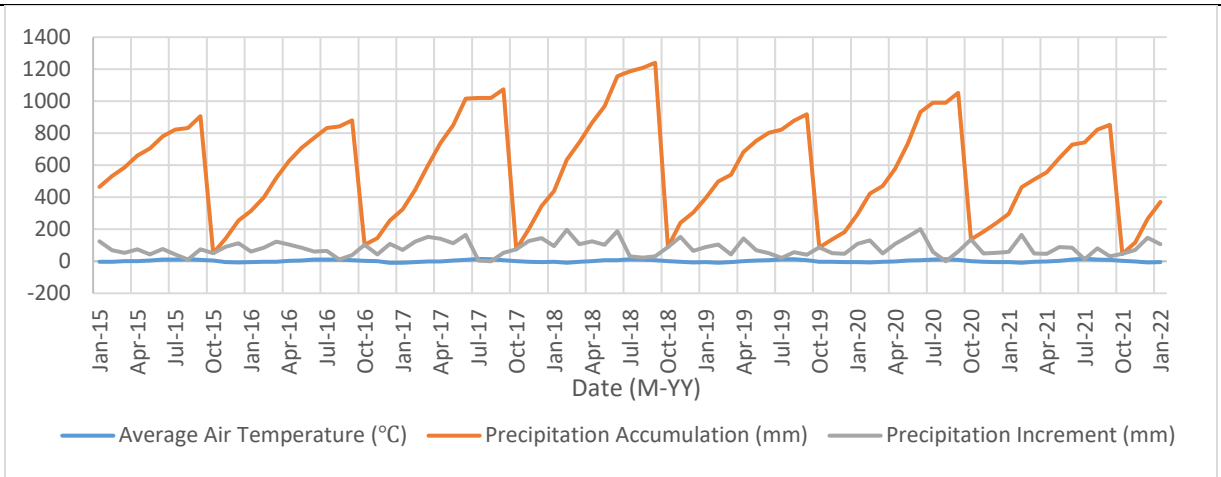

Figure 1: Precipitation accumulation from January 2015 to May 2022 at the Warm Springs, MT USGS monitoring station

The study area is dominated by 3 formations; the Cretaceous Boulder Batholith (Kg), the Miocene Six-Mile Creek Formation (Tsc), and Quaternary alluvium (Qal). The Tsc is subdivided in this area into the Big Hole River (Tscb) and Sweetwater Creek (Tscs) members.

Kg granite is the dominant unit in the upper section of the watershed. Kg is light to medium gray, or light brownish with a hint of pink with massive, jointed outcrops that form the Butte pluton, which is the principal pluton of the Boulder Batholith. The unit contains coarse, medium, and fine granites which exhibit normal-zoned, orthoclase, and quartz. Likewise, Kg granite contains accessory amounts of sphene, apatite, magnetite, and rare zircon, mafic minerals, which are largely altered to chlorite and epidote (Scarberry et al., 2019).

Tscs comprises the majority of slope walls to either side of the stream and some of the valley floor. This unit is poorly lithified, tan to light gray, immature silt, sand, and gravel with an ashy matrix. Clasts mostly derived from local granitic and volcanic bedrock from the Lowland Creek formation (Tlc). This unit also contains 5 to 60 cm thick beds of matrix-supported very coarse sand to pebble conglomerate with silty to sandy matrix, interpreted to be debris flow deposits and 0.1 to 3m thick beds of clast-supported pebble to cobble conglomerate, with sub rounded to rounded clasts of predominantly local affinity which are interpreted to be small to major channels. In addition, Tscs commonly includes 10- to 30-cm-thick massive light gray ashy silt to fine sand beds. Exposures are up to 360 m thick (Scarberry et al., 2019).

Tscb is a well-sorted, clast-supported, coarse sand to boulder gravel conglomerate with a sandy matrix. Clasts are rounded to well-rounded and commonly imbricated. This unit contains white, gray, pink, and red cobbles of Belt Supergroup quartzite, and biotite–muscovite granite, lithic sandstone, and schist derived from the footwall of the Anaconda Detachment. At the field site, Tscb thickness ranges to more than 120 m thick.

Alluvium (Qal) spans the valley floor in the bottom half of the of the field site. This unit is primarily clay, silt, sand, gravel, and bog deposits produced by or near channels of modern streams. Clasts are generally rounded and well sorted and are sourced from both local and distal units. Thickness of the Qal alluvium is generally less than 10 m but locally up to 60 m thick (Scarberry et al., 2019) which is likely the case for the lowest section of Reach 3 (Figure 2).

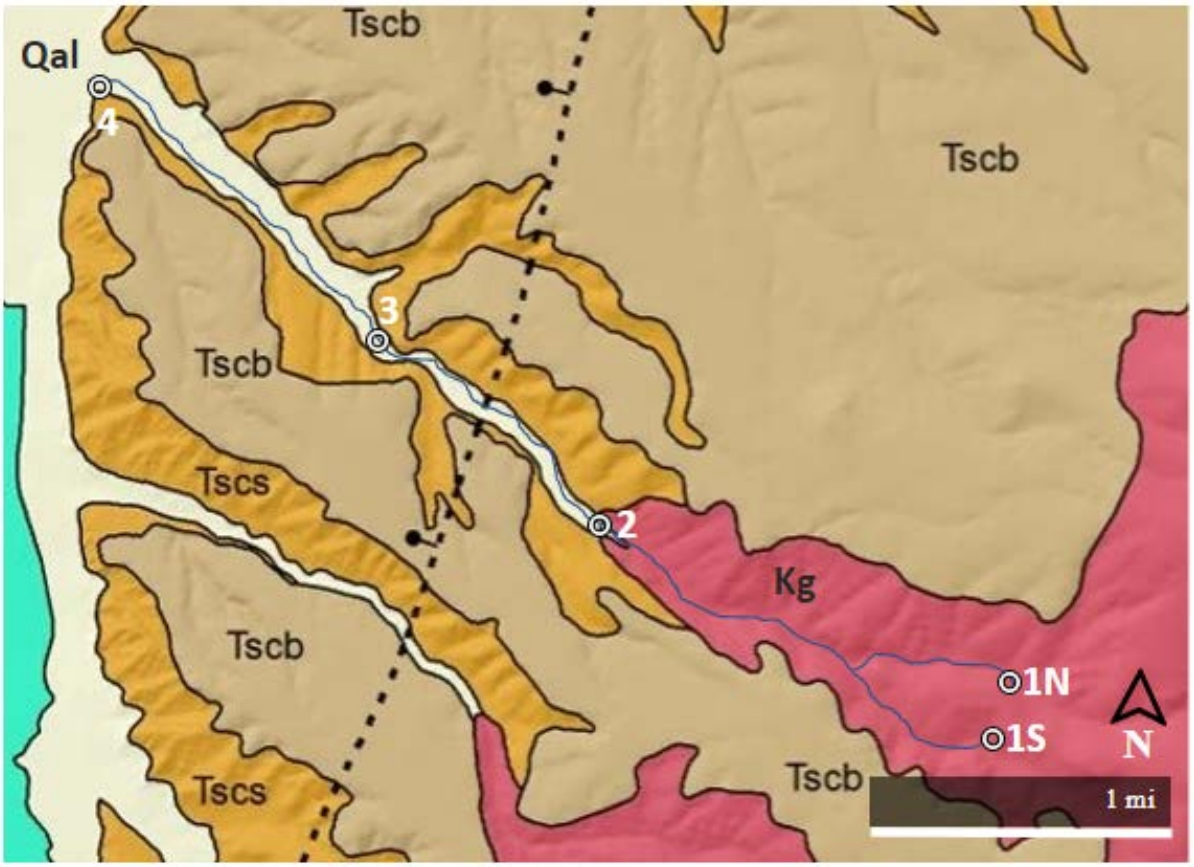

Figure 2: Geologic units at the field site include the Boulder Batholith Granite (Kg), the Sweetwater Creek (Tscs) and Big Hole River (Tscb) members of the Miocene Six-Mile Creek Formation (Tsc), and alluvium (Qal)

The study area can be summarized by five gauging sites that delineate three monitored reaches along the creek (Figure 3). Each site is coupled with a stilling well/staff gauge in the creek and one or two piezometers located on the creek bank.

Figure 3: The Perkins Gulch field area covers roughly 6.4 km of stream spanning from the northernmost extent of the Warm Springs Wildlife Management Area to United States Forest Service stations.

The uppermost site consists of two branches, the north fork and south fork, which feed the main Perkins Gulch stream. Sites 1 (1S) and 0 (1N) have stilling wells and piezometers. These areas are primarily forested valley in more mountainous terrain.

Site #2 is in a BDA-restored stretch and includes a stilling well and a piezometer. These BDAs have been blown out. The reach between sites 2 and 3 also contains remnants of abandoned beaver colonies consisting of both dams and valley-filled sediments from past beaver activity. This region is composed of woody debris and fine sediment. Sites 2 and 3 are separated by a narrow

bedrock notch where Tlc constricts the stream corridor. This area is covered by grasses, shrubs, and some low-lying woody vegetation.

Site #3 includes a stilling well and 3 adjacent piezometers. This area is largely bracketed by steep valley walls with sparse vegetation. BDA restoration was conducted in this area in the Fall of 2017. BDA structures in this reach are intact and appear to result in elevated stage and aggrading streambed.

Site #4 is the lowest monitoring site at the downstream extent of the study area. Two piezometers were installed next to the stilling well. This area includes very shallow valley to open plains and is best characterized as poorly consolidated fluvial plains with sparse vegetation.

Restoration at Perkins Gulch began in October of 2017 when BDAs were installed around sites 2 and 3. The landowner spent most of his life on the property and stated that the creek consistently ran dry in late-summer months up until 2019 and 2020, when the stream continued to flow year-round (Lampert, oral commun, 2021).

2.2. Reach Summary

Reach 1 is composed of two different tributaries that meet at the confluence to form the main Perkins Gulch stream. There was an unmonitored reach between Reach 1 and Reach 2, due to intervening private land. These tributaries were combined as reach 1, since they are both representative of headwaters conditions. The northern tributary (1N), has a 174 m elevation change over 2.6 km and the southern tributary (1S), has a 153 m elevation change over 2.4 km. Both tributaries are largely on USFS land that is used for grazing and recreation. Both tributaries are confined to narrow valleys with frequent outcrops of Boulder Batholith granite (Figure 2). Valley floors are covered by thick, organic rich soil which includes Qal along the stream bed. Both 1N

and 1S are in densely forested areas where Lodgepole pine, Douglas Fir, aspen, and shrubs and forbs dominate. Grasses are largely limited to stream banks and clearings. Dense vegetation and thick organic covering likely help with moisture retention and infiltration. Neither 1N nor 1S are restored using BDAs,

In Reach 2 there is a 69 m elevation change along a 1.5 km length of stream between sites 3 and 2. This reach is on DNRC property and is primarily used for grazing. Reach 2 is characterized by groundwater interaction with shallow bedrock, an abandoned beaver complex, some densely wooded groves, and BDA restoration. The geology of the reach is dominated by highly developed soils, tertiary and quaternary fluvium, talus/scree from the bracketing slopes to either side of the stream and some surrounding volcanics (Tlc; Figure 2). This reach contains dense vegetation that includes groves of cottonwoods, some aspens, and a variety of shrubs and grasses. Slopes are largely covered in conifers, increasing from site 3 to site 2.

Reach 2 contains two sections of BDAs with an abandoned beaver complex between them (Figure 4). Structures at and below site 2 have largely blown out. Qualitative increases in sinuosity and aggradation are evident near site 2. Near site 3 most BDAs are intact, and the stream bed has qualitatively aggraded. Separation of the stream channel from the floodplain generally increases from site 3 to 2.

Reach 3 is a 2.1 km long stretch of stream at the outlet of Perkins Gulch (Figure 3). The elevation drops 72 m over this reach. Reach 3 is on private property (Lampert) used primarily for grazing. It is characterized by a wide, shallow valley beginning immediately below the Tlc bedrock notch east of site 3. Sediment is primarily Tertiary and Quaternary alluvium and fluvium with poorly sorted clasts from local units upstream. Reach 3 was the first reach to run completely dry during the summer of 2021. According to the property owner, this reach often runs dry. Heavy

grazing along this reach has resulted in poorly developed soils and little vegetation. What vegetation has survived along this reach includes white sage, yellow rabbitbrush, and cheatgrass, all at or below 1-2 ft in height. Vegetation density and stream discharge increase moving upstream from site 4 to site 3 but channel/floodplain connectivity declines.

3. Methods

3.1. Site Setup

BDAs were installed in reach 2 by Great West Engineering in October 2017 (Figure 4). BDAs were constructed of locally sourced wood and branches to minimize introduction of foreign materials. The structures consist of wooden posts installed in a line perpendicular to flow, with branches interwoven between them. Additional sediment and organic matter naturally accrued behind them.

Figure 4: A BDA at Site 2 (left) and an abandoned beaver complex in Reach 2 (right).

Groundwater and surface-water monitoring instruments were installed during August 2020. Shallow wells at monitoring sites 3, 2, and 1S consisted of 1.5 m long, 2.5 cm diameter PVC pipes which were manually driven into the ground using a metal fence post pounder (Figure 5), with a metal drive rod inserted into the PVC. These shallow installations provide an open bottom completion approximately 1 m below ground surface. Wells at sites 3, 2, and 1S range from 0.74 m to 1.1 m belowground surface. At site 3 (Figure 6) three shallow wells were installed. The first two wells were too shallow to reach water and so a third was installed to supplement data.

Figure 5: Hand held post pounder used to install shallow wells at sites 4-1 (right) and YSI Pro30 conductivity meter used to determine specific conductivity, conductivity, and temperature.

At site 4, deeper wells were installed using a Geoprobe which produced 4 in. diameter boreholes. The two wells at site 4 were 3.5 and 9.5 m deep respectively and were constructed of 1.5 in. diameter PVC pipe coupled with 5 ft. sand pack screen, and bentonite fill to seal the annulus. The wells were installed in August of 2020 and were screened in a small (<2.5 cm.) thick perched aquifer which rests on < 2.5cm. thick silt layers. In addition, site 4 contained a deeper pumping well (GWIC ID 178939; TD = 108 ft bags) which was installed by the property owner prior to BDA restoration

All wells and staff gages were surveyed using handheld GPS and a level for determining relative elevations. Wells at each site are named alphabetically from upstream to downstream (Figure 6). Values such as well depth, stick up height and depth to water were measured manually using a Solinst water-level meter.

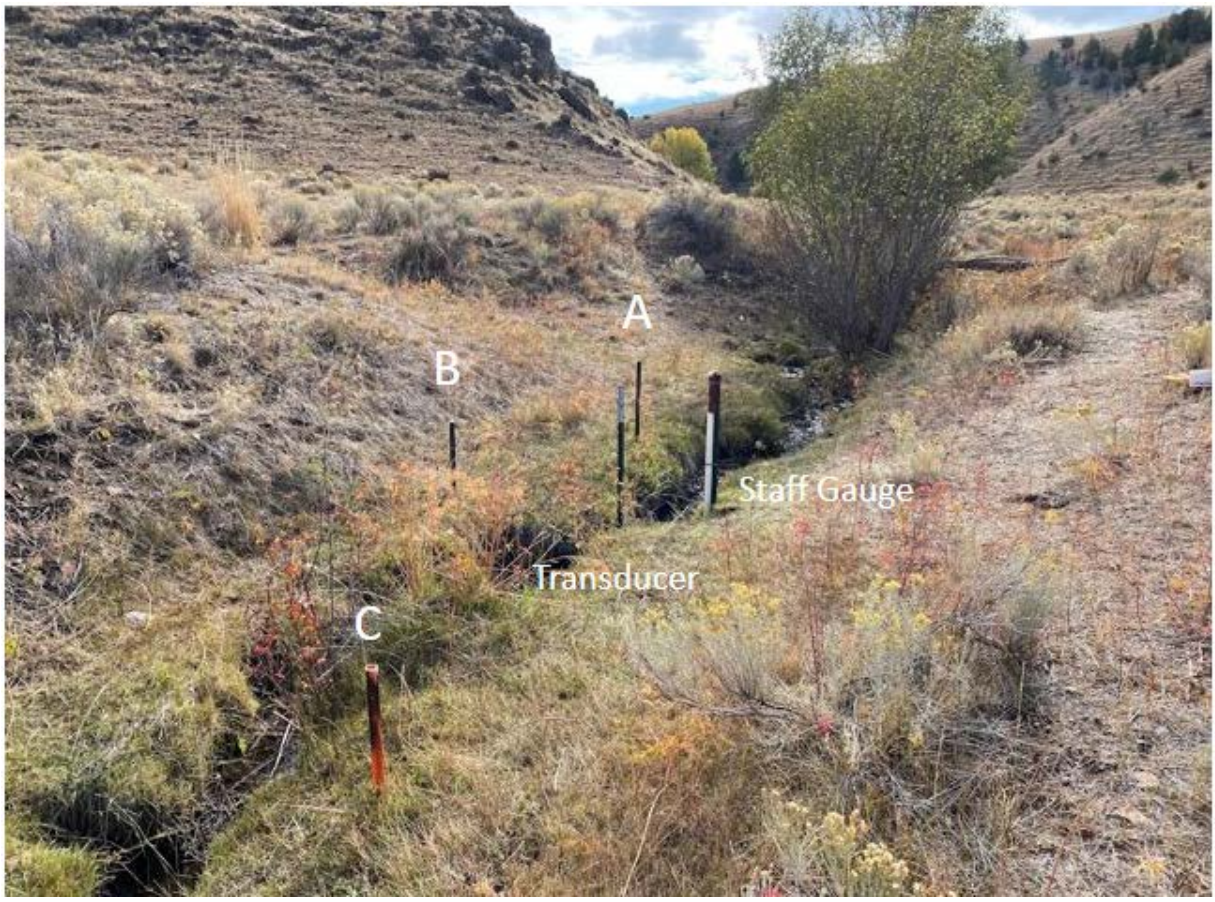

Figure 6: Groundwater monitoring site setup at Site 3. Wells at each site are labeled alphabetically from up to downstream.

Pressure transducers were installed in stilling wells but due to rapid sanding, erosion of stream banks, and shallow flows, data collected from these instruments were not used in the study.

3.2. Field and Analytical Measurements

Monitoring of the five field sites occurred weekly from early April to late May and then every other week/bimonthly from late May to late August 2021. Between April 2nd and October 9th, 2021, the site was visited on 13 occasions. During each visit, surface water monitoring consisted of salt tracer tests to determine stream flow, measurement of temperature, conductivity, and specific conductivity, and isotope sampling.

3.2.1. Groundwater Monitoring

Groundwater monitoring consisted of depth to water measurements using a Solinst water level meter. Measurements were taken from a standard point along the top of the well and were recorded in tenths of a foot.

3.2.2. Surface Water Monitoring

Stream temperature, conductivity, and specific conductivity were recorded using a YSI Pro30 conductivity meter. Temperature was recorded in degrees Celsius while conductivity and specific conductivity were recorded in microSemens per centimeter (μS/cm).

The salt slug tracer method (Winter, 2014) was used to determine flow rates during each site visit. All salt slugs were created by combining 125.5 g of NaCl and 874.5 mL of deionized water in a 1000 mL Erlenmeyer flask. The Erlenmeyer flask was sealed and shaken vigorously until all NaCl had dissolved into solution. The solution was divided into ten 100mL slugs stored in 125 mL HDPE plastic sample bottles. Each salt slug was sealed and labeled with date, contents, and intended site.

Tracer tests were conducted during each site visit, at each monitoring site. To ensure complete mixing during salt tracer tests, dilute rhodamine dye was injected at a standard point and allowed to flow downstream to a point where visual confirmation determined full mixing (Winter, 2014). Once the full mixing point was located, a conductivity meter probe was placed in the center of flow and background information such as conductivity, specific conductivity, and temperature were recorded. Then, without removing the probe, a 100 mL salt slug was injected at the rhodamine injection point. Beginning at injection and every five seconds after, specific conductivity was recorded until conductivity of the stream returned to background levels. This indicated that the entire salt slug had passed through the stream. Depending on velocity of flow and volume in the

channel, several tests were performed, and the best curve was selected to represent that date. Salt tracer tests were conducted from the farthest downstream site, site 4, to the highest site, sites 1S and 1N, to prevent any residual change in conductivity from impacting tracer test results.

Due to unusually dry conditions, there were many instances beginning in late May where flow was insufficient to support full mixing for the salt tracer method. In these cases, baseline information was still collected, and notes were made it to indicate that flow was either too low for testing or had simply ceased due to dry conditions.

Isotope analysis samples were collected at the baseline data point of each monitoring site before salt tracer tests were conducted. Water samples were collected in 8 to 10 mL borosilicate glass vials. Each vial was completely submerged in the center of flow and capped while underwater to avoid any inclusion of gases which could alter isotopic make up. Samples were labeled with monitoring site, date, and time of collection and stored in a refrigerated area to prevent evaporation. Samples were delivered to the Montana Bureau of Mining and Geology analytical chemistry lab and analyzed during December 2021 and January 2022.

3.2.3. High Resolution Field Exercise

A late season surface water balance (Appendix A.3.2) was conducted on August 22nd-24th, 2021 by collecting roughly 20 regularly spaced salt tracer test flows along reaches 1 and 2 (Appendix A.3.1). The results contributed to a high-resolution synoptic surface water balance and load balance (Appendix A.3.3).

During the same field exercise, soil samples were collected from 6 sites in reach 2. Samples were collected using a t-post and were stored in zip-lock bags labeled with location, date/time, and depth. Recovery ranged from 8 in to 58 in. Sample records include color, grain size, sorting, and

roundness. Moisture content and principal clay mineralogy were determined in lab analysis using a sediment oven and a PanAlytical TerraSpec HALO, respectively (Appendix A.3.4, A.3.5).

3.3. Data Analysis

Surface flows were determined using specific conductivity measurements from the monitoring sites and curve integrations from salt tracer tests. Flows were calculated using the salt tracer concentration integration method as outlined in Winter, 2014.

Temporal and surface water balances were conducted using baseline measurements collected at each motoring site. By comparing flow rates in upstream and downstream reaches of monitoring sites, net gain was quantified. For example, Equation 1 combines flows of an upstream reach, tributaries, and groundwater contribution to determine downstream flow.

$Net\ Gain = \ Q_{down} - (Q_{Trib.} + Q_{up})$	(1)

where Q_{up} is discharge from the upstream reach, Q_{Trib} is any flow contribution from tributaries to the main stream, Qdown is the flow at the downstream end of the reach, and *Net Gain* is the change in water volume from upstream to downstream, either positive or negative. At Perkins Gulch, the watershed contains one main stream which results from two tributaries (Reaches 1N and 1S). Reaches 1N and 1S were treated as a combined reach rather than tributaries for water balance calculations. Since both down and upstream discharge could be measured, and no tributaries contribute to flow, the only unknown in the equation is *Net Gain*.

Negative *Net Gain* values indicate a losing stream, and a positive value indicate a gaining stream.

A load balance was used to estimate specific conductivity values for groundwater which were later used in 2 component mixing calculations. Conductivity of groundwater was calculated from surface conductivity and calculated groundwater discharge using the following derivation.

$$Q_{up}C_{up} + Q_{gw}C_{gw} = Q_{down}C_{down} \quad (2)$$

$$\frac{Q_{down}C_{down} - Q_{up}C_{up}}{Q_{gw}} = C_{gw} \quad (3)$$

where C_{up} is the specific conductivity of upstream flow, C_{down} is the specific conductivity of downstream flow, and C_{gw} is the specific conductivity of groundwater flow. Qgw is the calculated discharge to the stream from groundwater, which is assumed to be equal to the Net Gain.

To determine how and in what quantities surface and groundwater is mixing at the study site a 2-component mixing model was constructed using specific conductivity. For this calculation it was assumed that the combined fractions of near surface water and groundwater was 1. The equation 8 can be rearranged to determine the fraction of groundwater

$$f_{ns} + f_{gw} = 1 \quad (4)$$

$$f_{gw} = 1 - f_{ns} \quad (5)$$

where f_{ns} is the fraction of near surface water, f_{gw} is the fraction of groundwater, and 1 represents the sum of all water contained at the site.

The lowest recorded surface flow SC measurements (120 µs/cm) was selected for near surface/overland flow in two-component mixing measurements (Figure 9). It was assumed that this value would be the most representative to true overland flow. Likewise, reach averages from groundwater SC calculations were chosen to represent the SC of groundwater at each site (Appendix A.2.3, A.2.4, A.3.3). Like load balance calculations, conductivity was included in the equations to compare groundwater, near-surface, and surface flow. By substituting equation 8 for

the fraction of groundwater, the fraction of near surface flow was calculated and then back substituted to solve for the groundwater fraction.

$f_{gw}C_{gw} + f_{ns}C_{ns} = C_{stream}$	(6)
$(1 - f_{ns})C_{gw} + f_{ns}C_{ns} = C_{stream}$	(7)
$C_{gw} - f_{ns}C_{gw} + f_{ns}C_{ns} = C_{stream}$	(8)
$f_{ns}(C_{ns} - C_{gw}) = C_{stream} - C_{gw}$	(9)
$\frac{C_{stream} - C_{gw}}{C_{ns} - C_{gw}} = f_{ns}$	(10)

4. Data and Results

4.1. Surface Water

Water year 2021 was dryer than average, with a total precipitation accumulation of 853 mm at Warm Springs where median annual precipitation of 1,026 mm/yr. Reduced snowpack and rainfall contributed to drought conditions across the state and may have resulted in lower-than-normal flows at Perkins Gulch. In early May, flows peaked between 20-56 L/s. By late May, flows at site 4 were recorded as 0 L/s. By the end of the study period in late August, only monitoring sites 1S and 1N retained measurable flow at a combined rate of 8.2 L/s (Figure 7). Site 3, which is at the bottom of BDA restored reach 2, maintained measurable flows until early August but later ran dry.

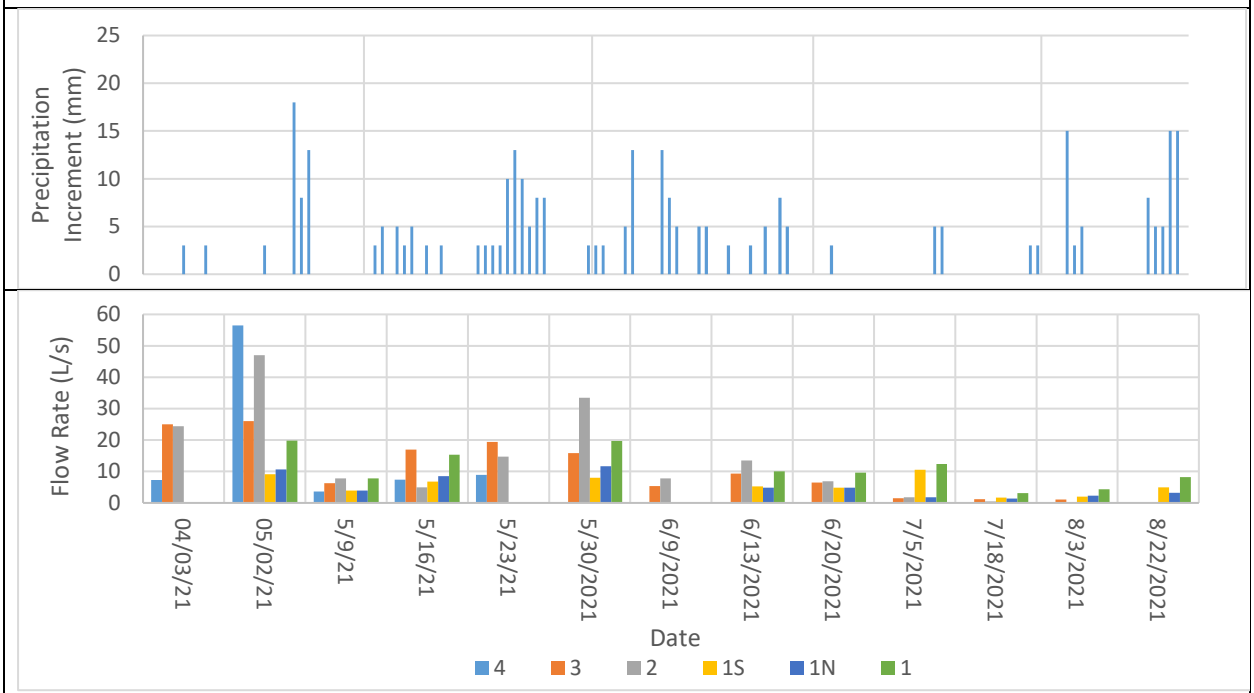

Figure 7: Precipitation increment in millimeters (top) and surface flows at Perkins Gulch (bottom). Surface flows peaked in early May but by the end of that month several monitoring sites recorded flows of 0 L/s.

Precipitation events occurred before May 2nd and 30th with 39 mm and 53 mm of accumulation, respectively. As such, noticeable peaks in surface flow were noted on both dates.

Surface flow temperature generally trended upwards over the 5-month field study with the exception of two outliers at 19.9 ℃ on May 16th and 2.6 ℃ on May 23rd. Maximum and minimum recorded surface flow temperatures are congruent with daily average air temperatures on those days, which were recorded at Warm Springs as 18.9 ℃ and -0.8 ℃, respectively. Despite these outliers, surface flow temperature generally increased from about 6 ℃ in early April to about 16 ℃ in early August., From April to August the daily average air temperature increased from 0 ℃ to 18 ℃ (Figure 8). The last surface flow temperature at Perkins Gulch was recorded on August 22nd but daily average air temperature did not drop below freezing until October 9th.

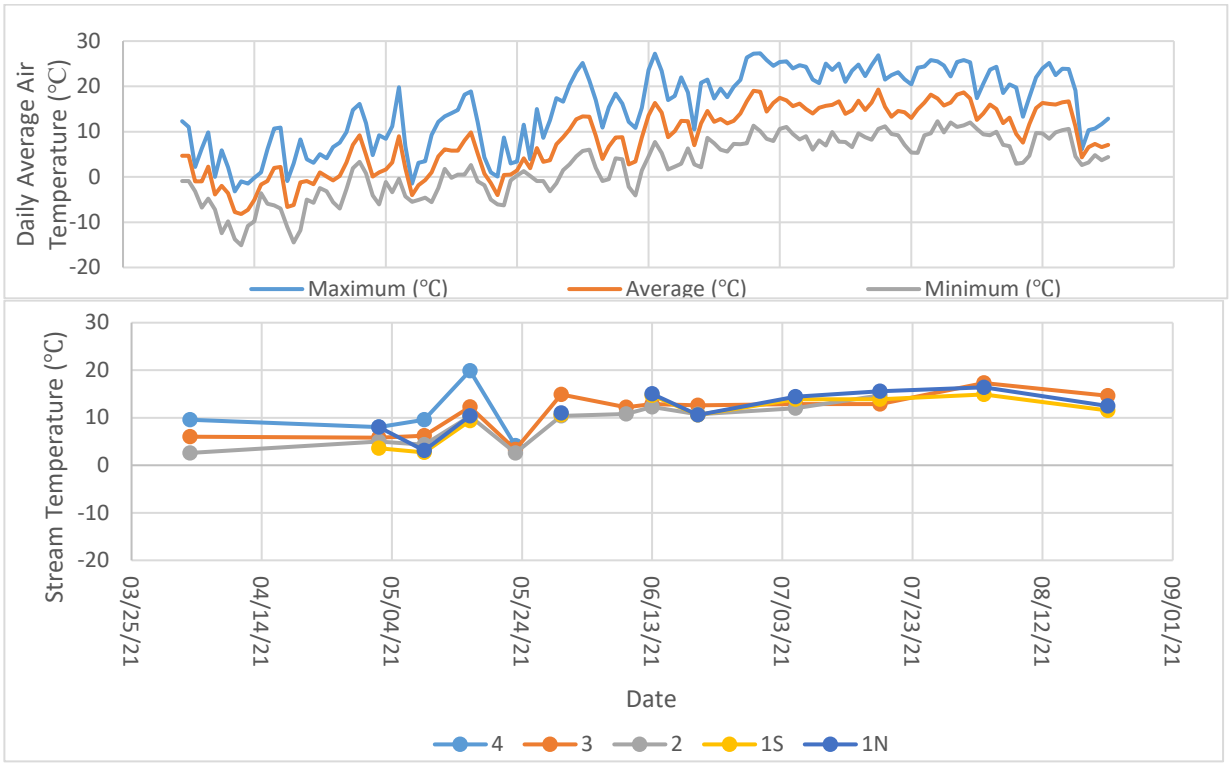

Figure 8: Air temperature at the Warm Springs USGS weather station (top) compared to surface flow temperature at monitoring sites 4-0 (bottom) over the course of the 5-month field study.

While distinct patterns were noted for both surface flow and temperature, specific conductivity of surface flows remained at a relative constant 330 µS/cm for all sites during the study period. Outliers include May 9th, May 23rd, and July 5th. Minor precipitation events occurred on May 9th and July 5th with 5 mm and 3 mm of precipitation, respectively. An event with a total of 13 mm of precipitation occurred on May 23rd. The overland flow from these precipitation events may have resulted in increases in specific conductivity and discharge (Figures 7, 9) and a decrease in temperature (Figure 8).

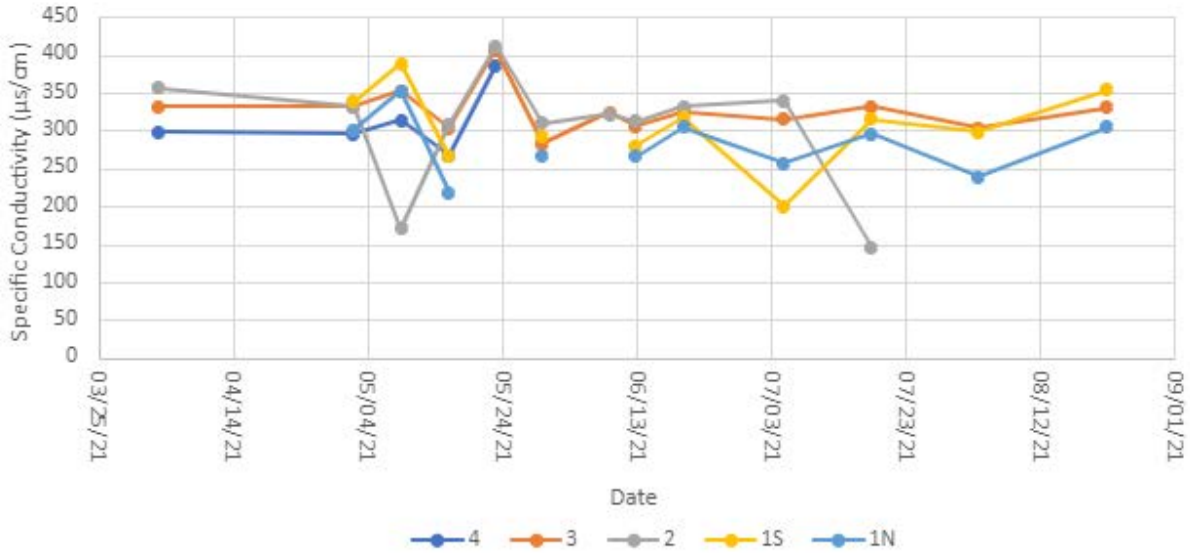

Figure 9: Specific conductivity of surface flow at monitoring site 4-0 over the course of the 5-month field study.

4.2. Groundwater

Groundwater levels declined rapidly at Perkins Gulch. Site 1S was the only site with measurable groundwater by the end of field season in late August (Figure 10). The last water measurements at site 4 were recorded on May 23rd, site 3 on April 4th, and at site 2 on July 18th.

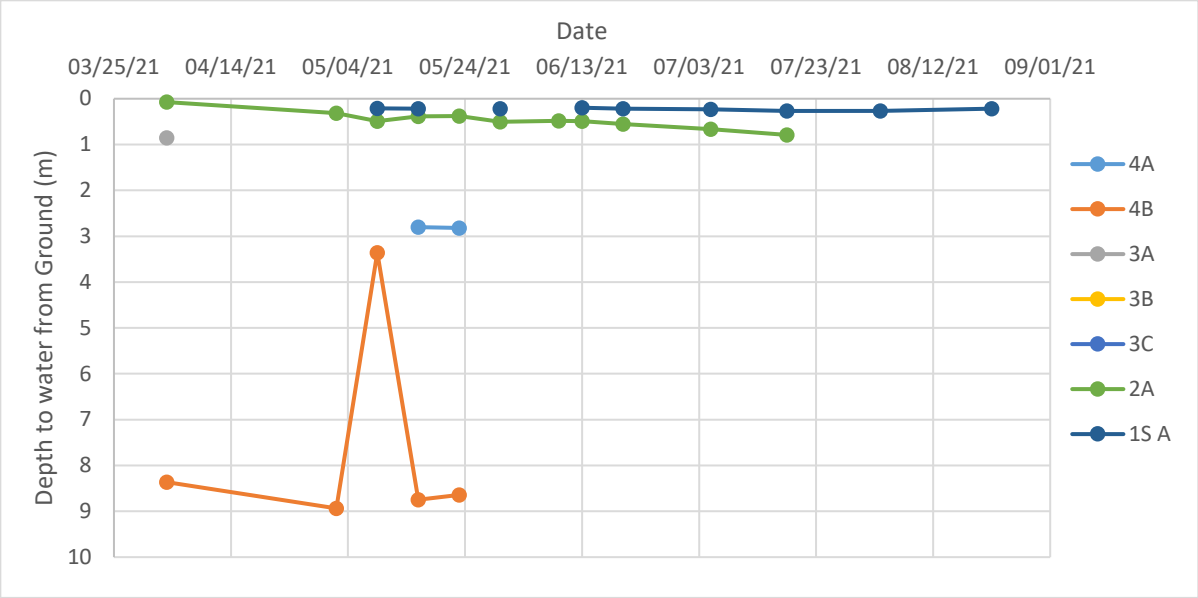

Figure 10: Groundwater level gradually declined from early April to the end of August. By the end of the field season well A at site 1S was the only well to retain measuarable groundwater.

Wells at site 3 were dry for the entire study. Wells at site 4 went dry in late May, despite being the deepest monitored wells in the study area (up to 9.6 m bgs).

4.3. Surface Water Balance

In reach 1 the maximum measured stream gain was 27.2 L/s, and the maximum loss was 10.4 L/s. At reach 2 maximum gain was 12 L/s and loss was 21 L/s. Reach 3 was losing for the entire study with minimum loss of 1.1 L/s and a maximum loss of 26 L/s (Figure 11). Since flow was zero at the lower end of reach 3 after mid-June, losses after that time are limited by the amount of water flowing into the upstream end of the reach.

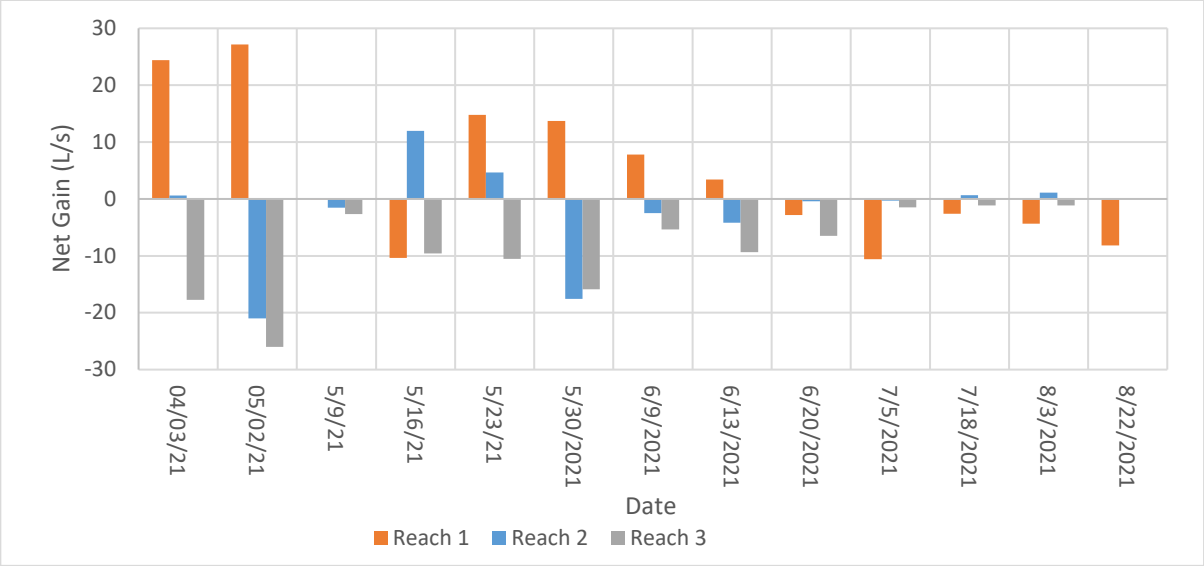

Figure 11: Net gain/loss as calculated from the surface balance over the 5-month study period. Negative values indicate that the stream is losing, while positive values indicate gaining.

Reach 1 was strongly gaining from early April to mid-June, with a brief losing period from early to mid-May. Reach 1 showed net losses from mid-June through the end of August. Reach 2 was a losing system but briefly transitioned to show a net gain from early to mid-May, and weakly gained after mid-July. Reach 3 was a losing system throughout the study period. Overall, groundwater systems at all three reaches converged on a neutral gaining/losing status. Reduced groundwater contribution in the reaches is likely partly due to dryer summer conditions over the course of the study (Figure 7).

4.4. Load Balance

Groundwater specific conductivity at each reach was calculated using the stream specific conductivity, stream flow, and the net difference in flow along each reach. This assumes that groundwater is the only source of water for gains, and that surface inflows and soil water are negligible. Similar to the SC of the stream water (Figure 9), the calculated SC of groundwater remained at a relative constant between about 300 and 400 µS/cm throughout the study, but with several noticeable deviations (fig. 12). The maximum calculated groundwater SC was 664 µS/cm

in reach 2 on April 3rd, while the lowest calculated was 209 µS/cm in reach 1 on July 5th (Figure 12).

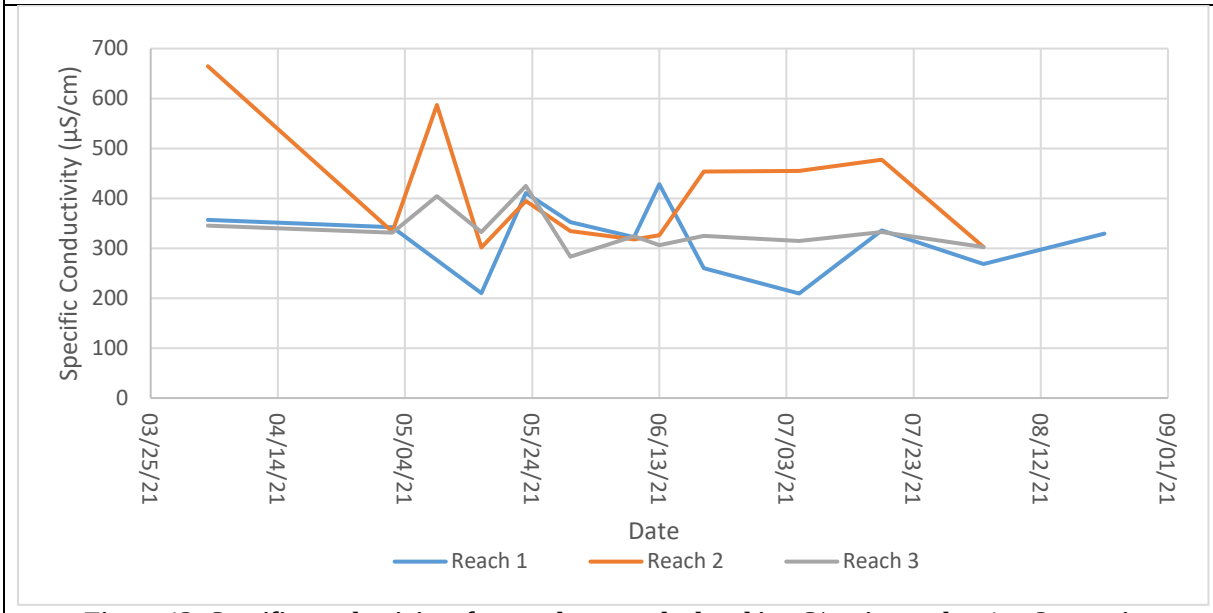

Figure 12: Specific conductivity of groundwater calculated in µS/cm in reaches 1 to 3 over time.

A steep peak in SC was calculated on May 9th in reaches 2 and 3. A precipitation event occurred on May 9th which may have contributed to deviations surface and groundwater SC. Another source of the peak may be high SC surface water inflow. The average calculated groundwater SC for reaches 1, 2, and 3 were 320 µS/cm, 410 µS/cm, and 340 µS/cm, respectively.

4.5. Two-Component Mixing

A two-component mixing model was developed to calculate fractions of overland and groundwater flow. In general, discharge of the two components increases upstream, but discharge decreases dramatically over time regardless of location in the watershed (Figure 13).

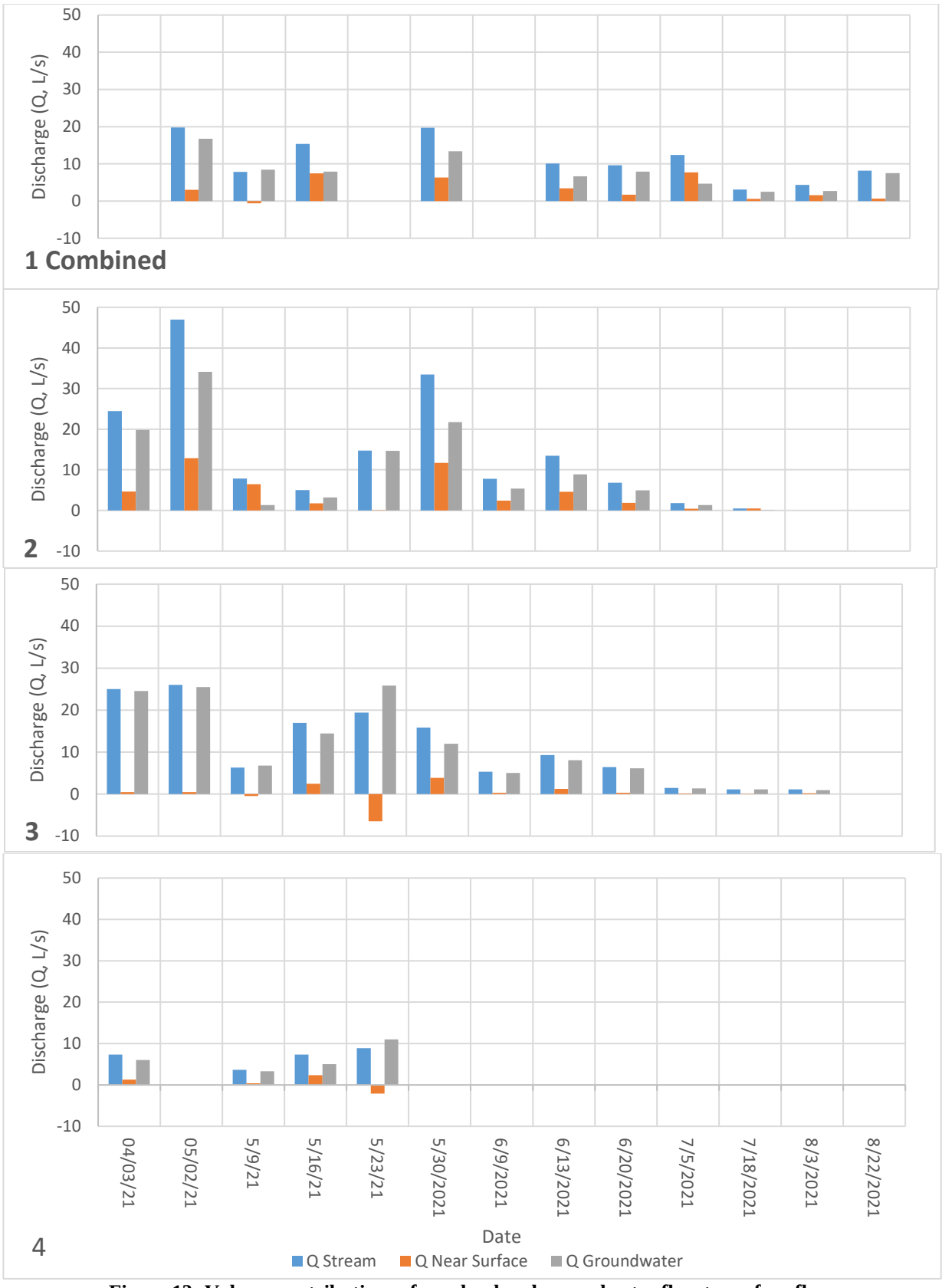

Figure 13: Volume contributions of overland and groundwater flow to surface flow

For all monitoring sites, groundwater contributed the greatest volume to stream flow. The two-component mixing model was congruent with observed patterns of surface flow. By the end of the study, in all sites except for 1S and 1N ("1 Combined" in Figure 13), surface and groundwater discharges were calculated as 0 L/s.

Combined surface, overland, and groundwater flows at sites 1N and 1S were less than those observed at site 2 (Figure 13, 7). This may be a result of private wells in the unmonitored section of stream between the confluence and site 2.

Negative near surface discharge values were calculated at sites 2, 3, and 4 on May 23rd (Figure 13). It is unlikely that near surface flow flowed in the wrong direction that day, so the outlier value was a result of the averaged SC values for groundwater. On May 23rd surface SC at sites 2, 3, and 4 were recorded at 411 µS/cm, 407 µS/cm, and 386 µS/cm. The two-component mixing model compared these values to average groundwater SC values calculated from the load balance which were 335 µS/cm, 374 µS/cm, 365 µS/cm. Since groundwater SC was less than surface water SC, comparison of the two and near surface flow produced negative fractions of near surface flow and thus negative discharges. A precipitation event occurred on May 23rd which may have increased infiltration and thus forced an influx of longer residence time groundwater into the stream.

4.6. Isotopes

A total of 49 isotope samples were collected from the five main monitoring sites over the course of the field study. Stable isotope analysis produced values for $\delta^{2}H$ and $\delta^{18}O$ in units of per mill (per thousand, ‰) relative to VSMOW (Figure 14).

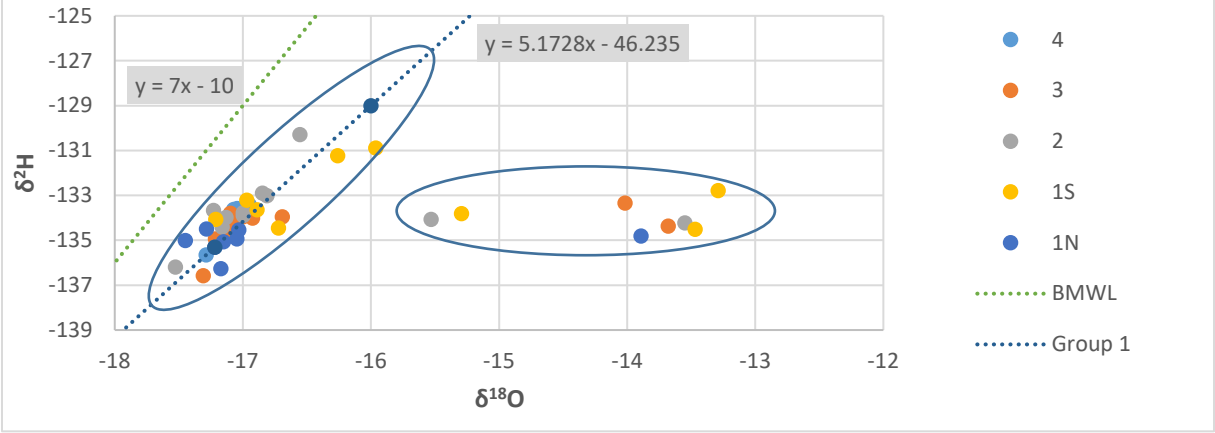

Figure 14: Stable isotope samples for δ^2H and $\delta^{18}O$ in units of per mill (per thousand, ‰) were compared to the BMWL (Gammons, 2006).

When compared to the Butte Meteoric Water Line (BMWL), two main groupings of samples are observed. The first group (group 1 on Figure 14) shares a positive slope with the BMWL but is 26% more shallow and is offset in the positive $\delta^{18}O$ direction. The second group (group 2 on Figure 14) is a cluster of samples that lay between -13.3‰ to -15.5‰ $\delta^{18}O$ and between -132.8‰ to -134.8‰ δ^2H. Samples in the second group are from early-May to late-June.

$\delta^{18}O$ and δ^2H values were also compared over time. In general, $\delta^{18}O$ of all monitoring sites remained constant over time at roughly -17‰. However, all five monitoring sites increased to -14‰ at some point between early May and early July (Figure 15).

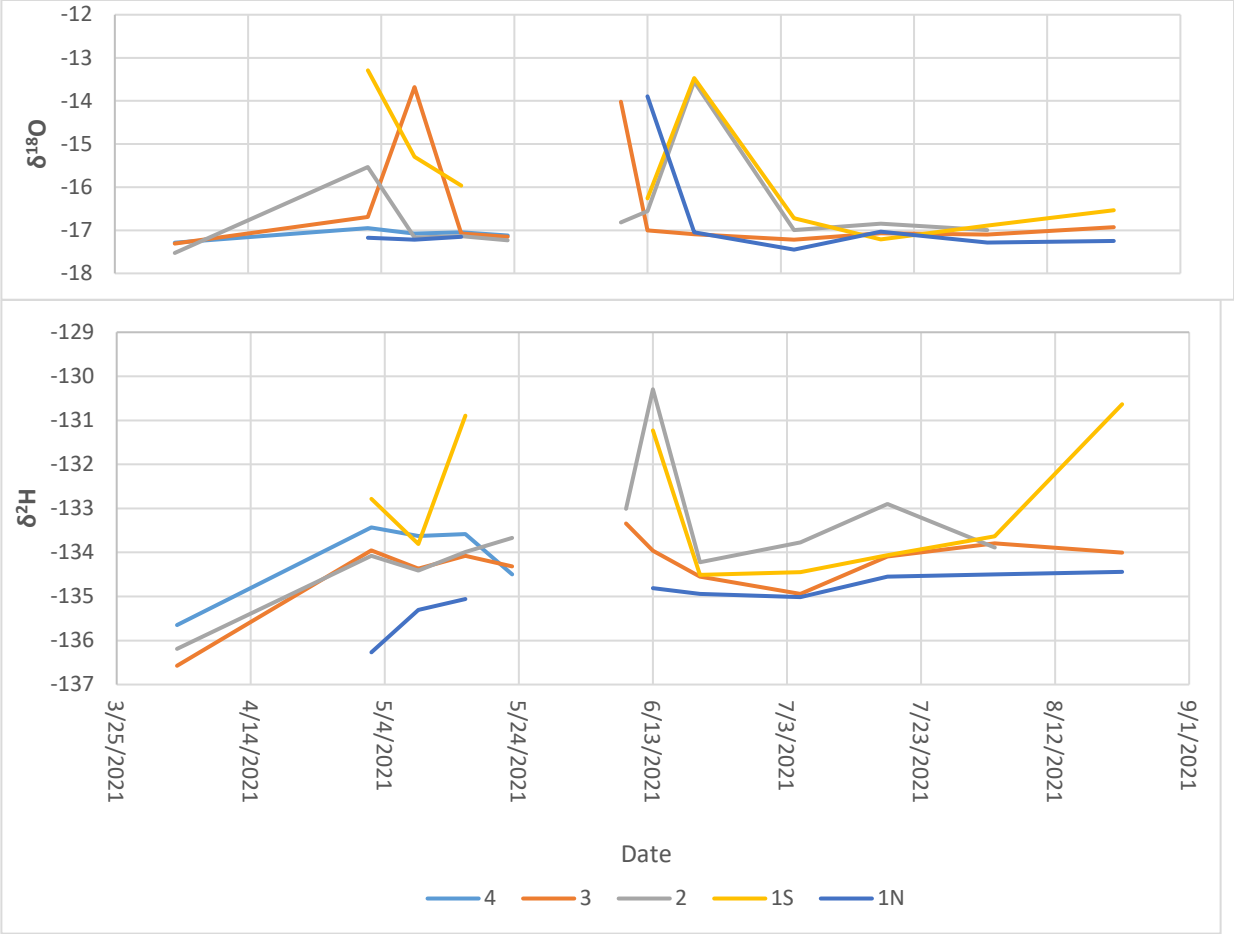

Figure 15: Surface water O18 and Deuterium over time

In contrast, deuterium values trended generally upward from -136 ‰ in early April to134‰ in mid-August. The maximum deuterium value observed was -129‰ at site 2 on June 13th.

When compared over time, $\delta^{18}O$ and $\delta^{2}H$ values at site 1S behaved in a cyclical pattern (Figure 16). Over the study period surface water at site 1S swung between less negative to more negative $\delta^{18}O$ and $\delta^{2}H$ values several times.

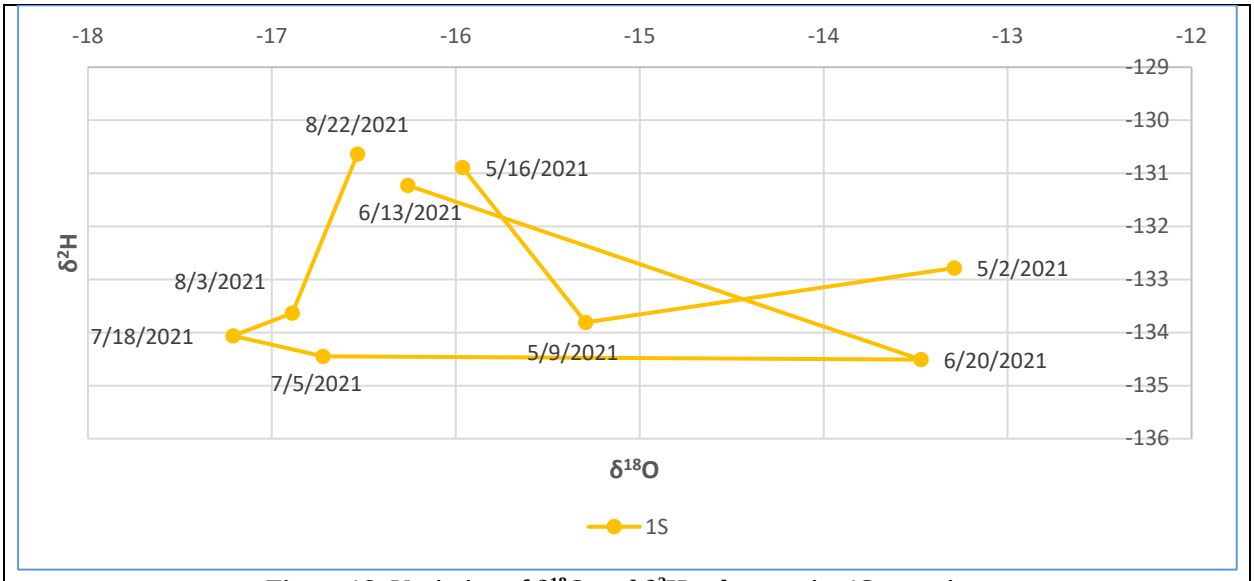

Figure 16: Variation of $\delta^{18}O$ and $\delta^{2}H$ values at site 1S over time

Minute changes in local climate or surface water/ groundwater interactions into the late season may be responsible for the cyclical trends in isotopic makeup at site 1S.

4.7. Spatial Variations

4.7.1. Late Season Flow Status

From August 3rd to 5th, a series of 16 sub-sites were selected to determine spatial variations of surface flow. By this time reach 3 was completely dry and so reaches 1 and 2 were the focus of the high-definition exercise. Status of flow (dry vs. flowing) was highly variable, with some regions of flow bracketed by dry stream, and vice versa (Figure 17).

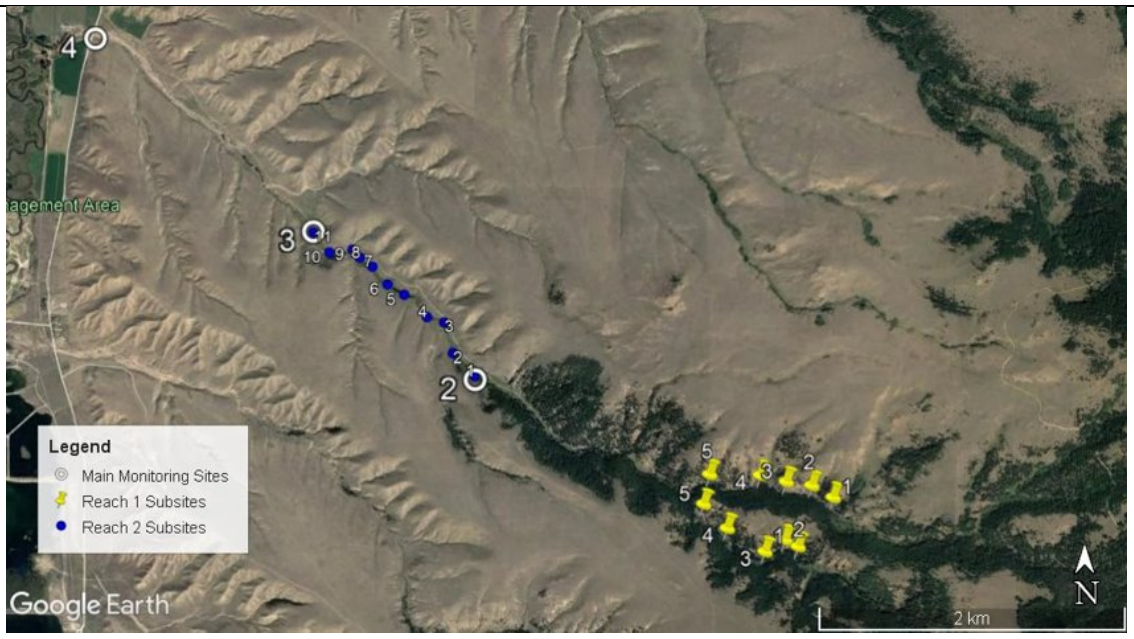

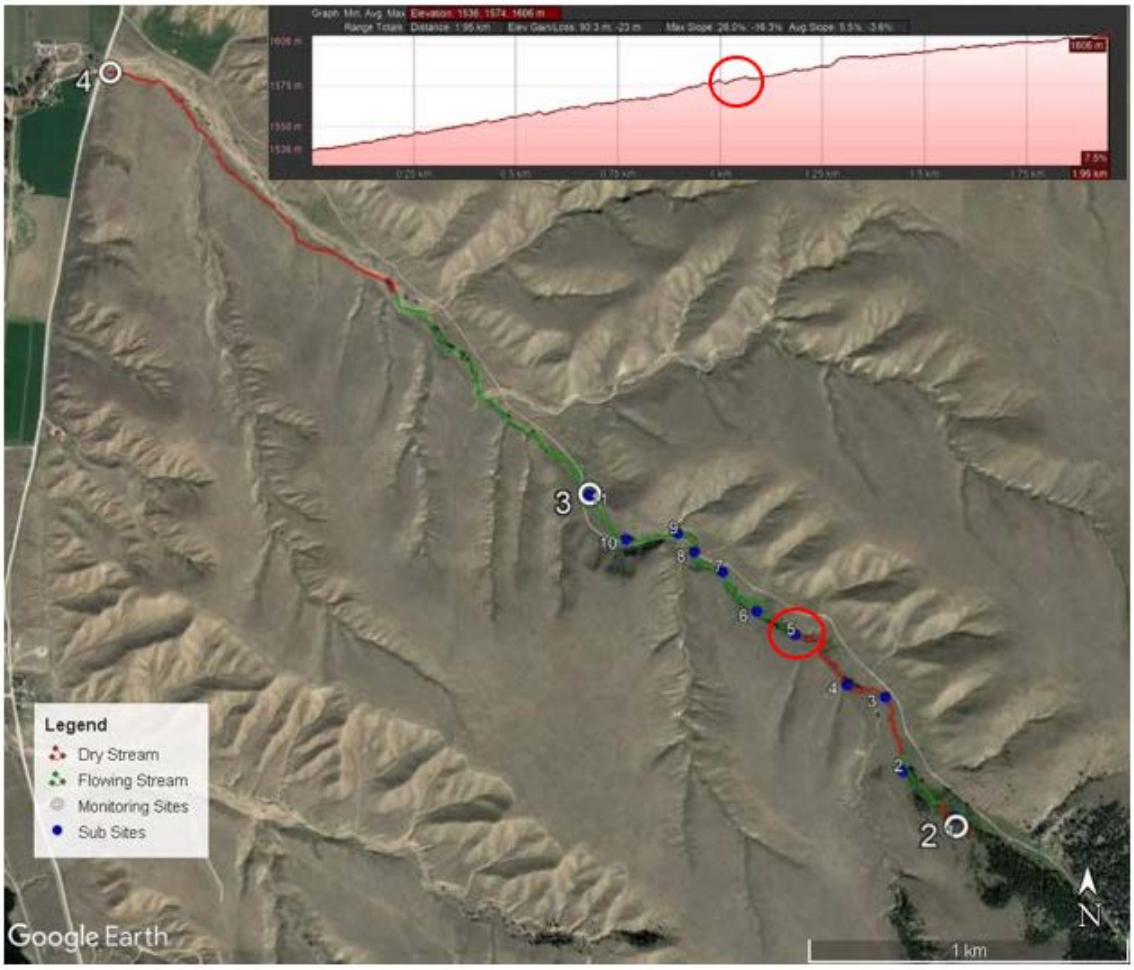

Figure 17: Late season subsite locations in reaches 1N, 1S, and 2 (top) and regions of measurable and dry flow during the August 3rd-5th field exercise Red circles indicate changes in stream grade that relate to changes in flow status.

4.7.2. Stream Flows Rates

A water balance was completed to supplement the observations of changes in flow status (Figure 18). From upstream to downstream (subsites 1 to 5) surface flows in reach 1 combined declined from over 4L/s at subsite 1 to less than 3 L/s at subsite 5 with a brief increase in flow at subsite 4. No trends in stream flow rate in reaches 1N and 1S were noted (Reach 1, Figure18).

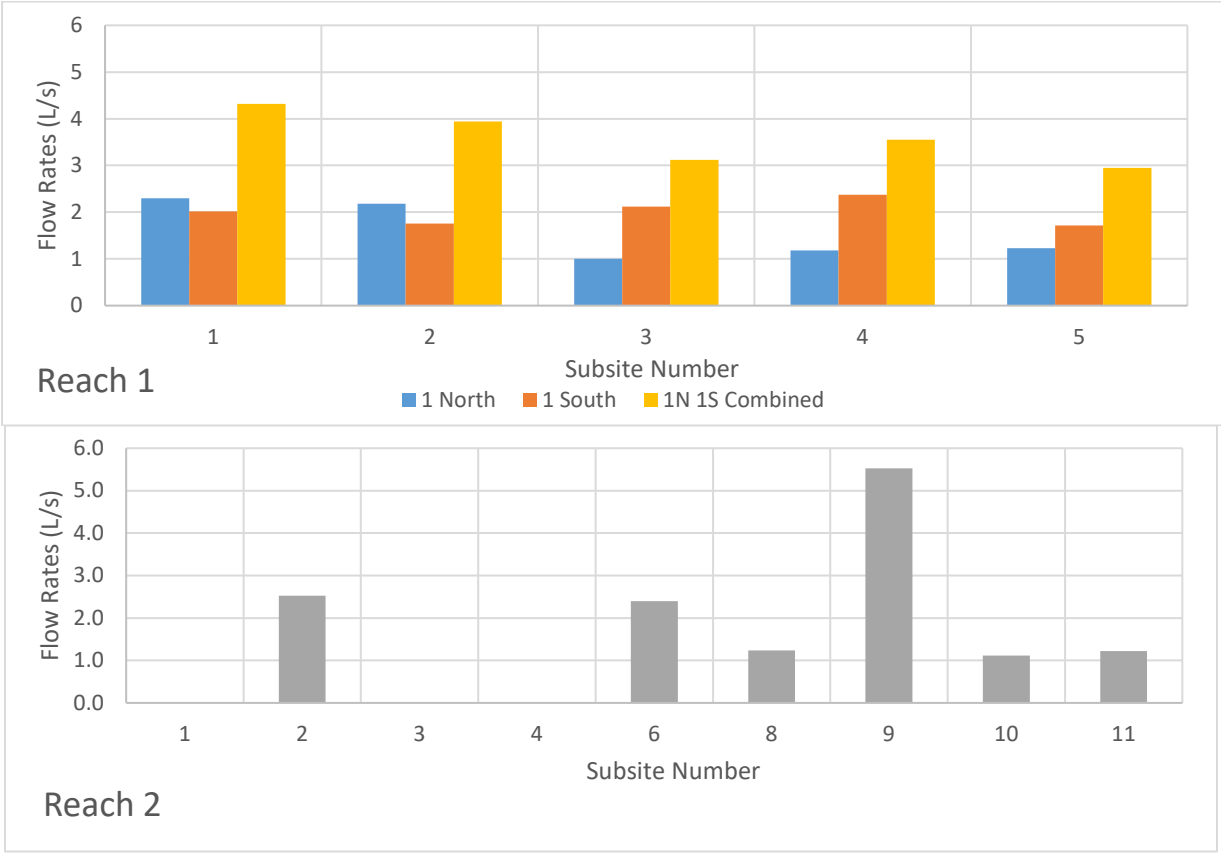

Figure 18: Stream flow rates at late -season subsites in reach 1 (combined 1N and 1S) and reach 2.

The temporal surface balance (Figure 11) established reach 2 as losing throughout the study season. However, the reach transitioned from gaining to losing, and flowing to zero flow, several times from subsite 1 to 11 (Reach 2, Figure 18). The greatest gain in surface flow was noted at subsite 9, which is immediately upstream of the Tlc bedrock notch. Stream flow increased by over

4L/s from subsite 8 to 9, and then promptly drops back to baseline levels downstream of the bedrock notch.

4.7.3. Load Balance

In the late season study, specific conductivity of groundwater was calculated by comparing values over distance. In the combined reach 1, no clear trends in SC of groundwater were observed. In reach 2, SC declined from 310 µs/cm to 160 µs/cm between subsites 9 and 10. These sites are upstream and downstream of the bedrock notch. A drop in stream SC was also observed downstream of the bedrock notch.

4.7.4. Isotopes

$\delta^{18}O$ and $\delta^{2}H$ varied over distance and time. In the early season, $\delta^{18}O$ values were generally erratic over the 5 monitoring sites but by the end of the season values became more positive upstream, apart from site 1N. The same trend was noted for $\delta^{2}H$ values which became more positive upstream. For both $\delta^{18}O$ and $\delta^{2}H$ site 1S consistently had the highest values of all the monitoring sites whereas site 1N had the lowest values aside from site 4. Despite being in similar topographic and ecologic zones, sites 1S and 1N represent endmembers.

5. Discussion

5.1. Surface-Groundwater Interactions

5.1.1. Climate conditions

In water year 2018 BDAs were installed in the upper and lower sections of reach 2. Water year 2018 was a wet year with a total precipitation at the Warm Springs SNOTEL site totaling 1,237 mm (120% of median; Figure 1). In the summers of 2019 and 2020 the landowner reported continuous flow of Perkins Gulch to the Clark Fork River for the entire summer for the first time in his life. Water years 2019 and 2020 were near normal, with annual precipitation accumulations of 90% and 102% of median at the Warm Springs SNOTEL site.

During this study, water year 2021 was dryer, with the Warm Springs SNOTEL site accumulated 823 mm of precipitation (80% of median; Figure 1). Temperatures measured at Warm Springs during the study were also higher than usual, with the monthly average peaking at 15.9℃ in July (Figure 1) compared to 11.9℃ and 12.8℃ at the same time in 2019 and 2020 (SNOTEL). Snowpack resources began to dwindle early in the snowmelt season and several sections of Perkins Gulch were dry in late May. As a result of exceptionally dry conditions at the study site, the fraction of streamflow supplied by groundwater increased to the end of the study period (Figure 11).

Local climate is somewhat wetter and cooler in reach 1. Both tributaries of the reach were observed to have lower surface flow temperatures and contain dense conifers. Tributaries 1N and 1S retained some degree of snowpack later in the season and continued to flow through the study period (Figure 11).

5.1.2. Geology and Topography

A combination of local climate and hydrogeologic setting played a role in reduced surface and groundwater flows in 2021. Precipitation accumulation in the 2021 water year was low and reach 3 went dry early in the season while other reaches had low stream flows (Figures 7, 10).

Both tributaries of reach 1 maintained flow throughout the study period. They are confined by steep valleys with intermittent meadows, and these areas are underlain by the Bounder Batholith bedrock (Kg). The low hydraulic conductivity of the bedrock prevents substantial subsurface flow, but fractured zones may provide storage, so the stored water is forced to the surface. Surface discharge in this reach was highest during the snowmelt season and immediately after precipitation events.

Reach 2 was observed to have several alternating lengths of flowing and dry streambed during the detailed flow measurements conducted in August 2021 (Figure 16). At many of the flowing locations, both annual and perennial vegetation, such as willow, was observed. Some such examples are the abandoned beaver complex and the bedrock notch. At several locations with no flow dense riparian vegetation was decadent, perhaps due to drought conditions. Locations with steeper grades showed increased surface-groundwater interactions, and water table elevation was near the ground surface, so it was able to supplement surface flows. Where stream grade was low, stream flow velocity declined and depth to groundwater increased, resulting in greater stream losses which eventually caused stream flow to cease.

The uppermost section of reach 3 at monitoring site 3 is just downstream of the bedrock notch, which is a narrow bedrock outcrop (Tlc) that protrudes on both sides of the valley. Surface flows at site 3 continued to the end of the study period (Figure 7) but with the exception of one measurement in early April, wells at the site were always dry (Figure 10). One explanation for continued surface flow and low specific conductivity is that the Tlc acts as a bottle necking point

and supplies low SC water to the stream. Below the bedrock notch the alluvial sediments are relatively thick and permeable so groundwater levels are deep. Despite this initial net increase of surface flows at the upstream end of reach 3, a combination of local geology (high hydraulic conductivity) and shallow, wide channels caused the stream to run dry by site 4.

The alluvium underlying the lower portion of reach 3 is a coarse, poorly sorted deposit with grainsize ranging from fine sand to small cobbles (Figure 2). This material is likely derived from the Clark Fork River system in the main valley, rather than Perkins Gulch. Due the relatively large grain size of these sediments, they are more permeable than the materials found further upstream. Groundwater elevation dropped below 9.5m in late May (Figure 10) and as such, it appears that the minimal flow observed in this reach is due to high stream losses reulting from deep groundwater and high hydraulic conductivity. The private stock well at site 4 is 33m deep and reaches cobbles and gravel (GWIC ID 178939). This well has continuously produced water.

Because of shallow flow, wide channels, and little shading vegetation, surface-water temperatures in this reach were consistently high. These flow characteristics may contribute to high rates of direct evaporation from the channel which likely exacerbated low flow conditions in the lower portion of reach 3.

5.1.3. Vegetation

Depending on density, type, and maturity, vegetation can reduce local water resources via evapotranspiration (Goulden et al., 2014), shield flow from heat and resulting direct evaporation (Weber et al., 2017), and indicate and abundance or deficit of water availability. These impacts were observed throughout the Perkins Gulch catchment, especially in reach 2.

Despite sections of dry flow upstream of monitoring site 3 and complete cessation of flow at the reach 3 midpoint by midsummer (Figure 18, Image A,) surface flows at site 3 continued

throughout the field season. In both tributaries of reach 1 surface flow was continuous throughout the field study albeit declining. In reach 1 the elevation, local topography, and vegetation likely contributed to reduced surface temperature, which reduced evapotranspiration and evaporation.

In several locations flow was observed to stop at groves of large woody vegetation such as cottonwood or shrubs (Figure 4, Site 2). At these locations it is likely that evapotranspiration, direct evaporation, and leakage into the aquifer contributed to flow cessation. For example, in early August surface flows stopped and resumed in several locations along reaches 2 and 3 with varying degrees of vegetation density. The upper length of reach 2 is vegetated with large shrubs and trees and contains both the abandoned beaver complex and BDA restoration.

The density of trees and shrubs generally decreases from site 2 to 3, where it eventually becomes sparse between site 3 and 4 (Image A, Figure 18). Mature woody vegetation is largely confined to individual groves. Especially at site 2, high vegetation density and maturity likely contributed to early cessation of surface flows. Flows at the monitoring site, which is defined by a dense grove of mature aspen, ended in mid-July but were continuous roughly 100m downstream where woody vegetation was less dense. Surface flow at site 2 resumed in November after the first frost of the season, presumably due to the cessation of evapotranspiration. A similar occurrence was noted at the last grove of trees downstream of monitoring site 3 (Image A, Figure 18). While some vegetation may have assisted in lowering direct evaporation rates, evapotranspiration is a significant sink in local surface and groundwater resources.

Figure 19: Flow termination point (A), bedrock notch (B), and abandoned beaver complex (C) in reaches 2 and 3

Vegetation type and maturity served as proxy data for local water availability. Locations like above the bedrock notch (Image B, Figure 18) retained flow throughout the study season and contained groves of mature woody vegetation. This indicates that groundwater bottlenecking at this point has been historically continuous. The same process is observed at the abandoned beaver complex (Image C, Figure 18) and sporadic groves between the complex and site 4. However, severe die-off of woody vegetation at these locations indicates that in recent years water availability has declined. Decreased availability is most likely a result of prolonged drought conditions but may locally be attributed to continued natural degradation of the abandoned beaver complex and may be related to heavy grazing. The complex historically served as a significant source of surface and groundwater retention as indicated by density and maturity of now-dying woody vegetation.

In both tributaries of reach 1 surface flow was continuous throughout the field study albeit declining. Reach 1 is defined by narrow valleys with shallow granitic bedrock and dense, mature vegetation, particularly Douglas Fir trees. Despite sharing a similar vegetation profile with the upper portion of Reach 2, surface flows in this reach were continuous. A combination of elevation, local topography, and a tall, dense tree canopy, which all produce lower temperatures, may increase melting time for seasonal snow which provides alternate sources of moisture for the denser vegetation. This reduces the proportion of surface flows lost to evapotranspiration.

Vegetation may reduce surface flow temperature and the amount of direct evaporation, but observations and Perkins Gulch indicate that it more frequently acts as a surface and groundwater sink unless combatted by some combination of local geology and topography. However, vegetation was used a proxy to determine what locations along the stream historically retained sufficient surface flow to support dense woody vegetation.

5.1.4. Late-Season Surface Balance and Gaining/Losing Transitions

The three reaches at Perkins Gulch transitioned from gaining to losing several times over the study period. Reach 1 was strongly gaining in April and May but later transitioned to moderately losing beginning in mid-June. Reach 2 was a losing system from April to late June, when it began to gain slightly. Both reaches 1 and 2 briefly transitioned to losing and gaining respectively in mid-May. Reach 3 was strongly losing through the study period (Figure 11).

Temporal transitions from gaining to losing likely results from climate and dry conditions during the field study, but it is standard for even wet years in semi-arid regions to see decreases in stream flow during late summer periods, and infiltration of streams near the transition from bedrock to unconsolidated materials has been well documented (see Markovich et al., 2019 for a summary). Similarly, net losing to gaining transitions resulted from precipitation events (Figure

7). Of the three reaches, reach 1 had the longest period of gaining. This likely results from cooler surface temperatures, increased cover, longer snowmelt period, higher precipitation, and a thin and/or shallow aquifer which continuously fed the stream. In contrast, shallow channels, and deep groundwater resulted in losing conditions for reach 3 during the entire study

Reasons for transitions from gaining to losing and vice versa differed spatially. Sudden increases in stream grade and general changes in stream topography (Figure 16) may have caused the stream to switch from losing to gaining as depth to groundwater below the stream changed. Shallow stream grades reduce flow velocity which may increase infiltration and thus cause the stream to be losing. However, sudden increases in grade may cause the shallow aquifer to intersect briefly with the surface to produce a gaining section.

In the late season, high-definition study, the stream was dry from subsite 2 to 5 in reach 2. Flows resumed at sub site 6 where specific conductivity of the stream was 180 µs/cm, markedly lower than any other sub site in the study. On July 18th, a specific conductivity of 146 µs/cm was recorded at site 2, despite no similar values being recorded at other locations on that date. Between sub sites 5 and 6 there is a series of topographic jumps which may produce brief intersection of the shallow aquifer and surface flow.

During the late season study, several trends were noted at the bedrock notch above main monitoring site 3. Surface flow increased and specific conductivity declined immediately upstream of the notch at sub site 9, before returning to relative background levels downstream at sub site 10 (Figure 17). Likewise, surface flow temperatures decreased by almost a degree Celsius from sub site 9 to 10 (Appendix A.3.1). This appears to reflect a strong groundwater influx within this area.

A load balance was completed from subsites with measurable surface flow and between subsites 1 and 10 of reach 2, SC of groundwater was calculated at around 310 µs/cm. However, between subsite 10 and 11, which are directly downstream of the bedrock notch, SC of groundwater was calculated at 163 µs/cm (Appendix A.3.3)

Changes in geology may result in gaining/losing transitions as the stream flows into a greater or lesser hydraulic conductivity unit. An example of this is reach 3 where flows are present at the uppermost extent but quickly decrease and cease as surface geology transitions from fine clays to course alluvial materials.

5.2. Impacts of BDA Restoration

Although BDA restoration was limited to reach 2 and only began in 2018, both short- and long-term impacts propagated downstream and resulted in hydrologic, ecological, and geomorphic changes. The extent of these impacts vary in permanence and their exact lifespan is dependent on environmental characteristics such as climate, topography, and local geology.

Hydrologic benefits of BDAs are controlled largely by geology (i.e. connection of stream to aquifer and aquifer characteristics) and topography, and can be positively or negatively skewed by climate conditions. For example, clay rich sediments are less conducive to infiltration and groundwater storage than coarse sand. Therefore, a BDA installed in clay rich sediment may be less effective in increasing groundwater storage. As such, local geology must be considered when selecting BDA installation site to maximize hydrologic benefits. Similarly, benefits of BDAs reflect climate conditions: drought conditions will result in fewer surface and groundwater resources and reduced magnitude of BDA impacts.

5.2.1. Hydrology and Stream Morphology

The natural beaver dam complex and adjacent BDAs have changed surface flow, stream morphology, vegetation, and groundwater response. This includes changes in stream sinuosity flow diversity and depth diversity.

Beaver dams and BDAs produce rapid alterations in flow velocity followed by changes in stream morphology, surface/groundwater resource availability, and habitat diversity. At Perkins Gulch, BDAs installed in reach 2 produced noticeable increases in stream sinuosity, especially at monitoring site 2. In 2018 BDA structures at monitoring site 2 were installed perpendicular to flow along the relatively wide stream channel. By the beginning of the field study in the spring of 2021, the stream had eroded around the BDA structures. Despite no longer serving as a source of significant decline of stream velocity or increased stream stage, these BDA structures forced stream meander and thus increased local sinuosity. While this did not assist with the primary goal of the Perkins Gulch restoration, which was to store groundwater during snowmelt and enhance stream flows during late summer months, it did create more complex riparian and aquatic habitat.

Observations of stream morphology at monitoring site 2 likewise included changes in flow velocity both up and down stream of BDA structures. BDAs caused pooling upstream of the structure as well as increased velocity downstream. In several cases small waterfalls were formed. Pools upstream of the structures aided in accumulation of organic matter, aggradation of the stream bed, improved wetland connectivity, and increased nutrient availability. Flow diversity around the structures was similarly beneficial and may have aided in habitat production for small native wildlife such as insects and birds.

Many of the BDA structures in reach 2, especially at monitoring site 2, have blown out or been meandered around since installation in 2018. At these nonfunctional dams, stream flow either flows through the blown-out dams or completely circumvents them. There is evidence of stream

aggradation with accumulation of sediments since the structures were installed at sites 2 and 3. Highly erodible soils in reach 2 reduced stability of structures, and contributed to increased sinuosity.

In normal water years, surface flows in reach 3 have been consistently low or dry in the late season. The land owner communicated that the stream flowed continuously in 2019 after BDA restoration. Either the wet conditions in the 2018 water year or BDA restoration may have caused this. It is possible that surface storage from BDAs in reach 2 and upwelling of groundwater at the bedrock notch were sufficient to maintain stream flow year-round.

5.2.2. Vegetation Response and Accumulation of Organics

Increased vegetation was observed around BDAs at monitoring sites 2 and 3, and below the bedrock notch. In locations where dam structures caused pooling, vegetation density and diversity was markedly improved. Aggradation at BDA ponds decreased channelization, which improved local wetland connectivity. By spring of 2022 small groupings of willows were established at ponded dams below site 2. In addition, the north-western edge of the meadow at site 2, which is used primarily for grazing, is transitioning into a wetland. This transition has likely been a while in the making as clusters of large shrubs are present where water is pooled.

At sites 2 and 3, partially blown-out BDA structures created the equivalent of new point bars which increase sinuosity and trap organic material in the stream. Aggradation of the stream bed and increased nutrient content creates ideal zones for new vegetation which may serve as nursery plants for further development. Similarly, the highest soil moisture content was observed in sections of reach 2 that contained BDAs or were near the abandoned beaver complex (Appendix A.3.4)

5.2.3. Duration of impacts

The duration of the impacts of BDAs is extremely varied. Water table responses to installation of BDAs begin to immediately degrade after the dam is blown out or otherwise removed (Westbrook, 2006). Benefits such as vegetation and changes in stream morphology begin to degrade at blowout but at a much slower rate. In this case the abandoned beaver complex in reach 2 was used as a proxy simulation for well-established BDAs over a long period of time.

The beaver complex is densely populated with mature vegetation ranging from grasses to large shrubs and mature trees. The presence of trees at the complex indicates that the local site experienced an extended period of increased surface and groundwater resource availability. However, much of the woody vegetation at the complex has begun to die off. Qualitative observations of the complex, however, indicate that while wetland connectivity is still heightened from beaver activity, the stream has begun reclaiming a principal channel which has led to general increase in flow velocity and a congruent decrease in infiltration and sinuosity. These changes in flow patterns overall indicate general decline of surface and groundwater resources.

5.2.4. Recommendations for BDA Restoration at Perkins Gulch

Site 3 is composed of a fine sediment matrix and any potential aquifer at the site is likely small and shallow. Future studies will need to include soil analysis to allow understanding of aquifers and when one might need to go back and redo structures. However, since flows continue at reach three, surface water storage may be sufficient to release some water during low flow period and contribute to continuous annual flow.

Many of the dams at Perkins Gulch have been completely and partially blown out. In order to mimic and maximize the benefits of natural beaver dams it is necessary to repair damaged dams and install additional structures. Installing main structural poles at depth in the stream and

extending the structure past the banks of the stream may help in postponing erosion around the structures and blowout. By creating complexes of BDAs and committing to continuous repair, hydrologic and ecologic benefits can be extended for floodplain development to reach a self-sustaining level. At Perkins Gulch it is likely that local geology beginning at the bedrock notch and extending to monitoring site 4 prevents significant improvement of surface groundwater connectivity. Similarly, any BDAs installed at the site will likely require periodic repair to support extended benefits.

Best practices for BDAs, including construction, dimension, and regional usefulness, have been largely outweighed by studies focusing specifically on post installation impacts (Pilliod et al., 2018). Impacts such as volume of BDA pools are mainly controlled by structure dimensions, local geology, and stream size. According to Wade et al. in 2020, stark differences in hyporheic zone processes were observed for BDAs of differing sizes, suggesting that hyporheic exchanges are dependent on BDA dimensions. As such, BDAs may only alter groundwater–surface water interactions after a threshold hydraulic step height is exceeded.

Likewise, the duration of surface/groundwater interaction post BDA installation is dependent on the structure's lifespan. Many of the BDAs at Perkins Gulch have been blown out or otherwise rendered non-functional and so responses in surface and groundwater resources are diminished. Determining best construction practices to prevent frequent blow-out is critical to ensuring long-term hydrologic impacts persist. For example, in a study by Pearce et al. in 2021, after one year only BDAs built around fence posts inserted into the stream bed with a percussion fence post driver were fully intact. Assuming long term increases in surface and groundwater resources are the primary goals of restoration, structures must be either consistently repaired or built with endurance in mind. However, short-term data indicates that BDAs can be used as a

stream restoration practice to reduce bank erosion and increase channel heterogeneity (Pearce et al., 2021).

6. Conclusions

In the last several decades BDAs have been widely utilized in regions both with and without historical natural beaver activity. The magnitude of benefits of BDAs is directly tied to landscape characteristics such as topography, geology, and hydrology. According to Pilliod et al. in 2018, the scale at which BDAs have been implemented vastly outweigh guideline studies for best practices. And as such, additional analysis on appropriate construction and geologic/climate regions for placement are needed.

If late season stream flow through the site is the primary goal of restoration additional high resolution, geologic analysis is needed at each of the main monitoring sites. Site 1N, 1S, and 3 are bracketed by bedrock walls but flowed throughout the study. It is possible that any aquifer contained in those reaches is shallow. Simple core analysis would help determine depth and thickness of aquifer as well as aid in conductivity calculations for the sediment in the area. Erodible soils at site 2 caused BDA structures to rapidly fail and stilling wells to fill. Likewise, it is suspected that vegetation played a key role in reducing surface and groundwater resources throughout the growing season. Soil analysis of stream sediments would allow for additional calculations of groundwater velocity and hydraulic conductivity while a detailed vegetation study would help in determination of water lost to evapotranspiration. Since site 4 ran dry early in the season, and had historically followed the same trend, it is possible that surface flows are infiltrating in the alluvial material and in a deep aquifer. Additional wells and core analysis (including the private well at site 4) would confirm the depth and thickness of the aquifer in the reach.

Both high and low precipitation accumulations were observed at Perkins Gulch prior to BDA restoration in 2018 but continuous flow at site 4 was never observed. However, in water years 2019 and 2020 the stream flowed continuously through site 4. Regardless of water

year magnitude or local geology, BDA restoration likely contributed to continuous flows in those years. By the start of the field study in 2021 most of the structures were either completely or partially blown out. To resume restoration development, all the dams in reach 2 need to be reinforced and repaired. Additional structures in reach 1, on the unmonitored private property in reach 2, and in the abandoned beaver complex may improve surface and groundwater storage as well.

In addition to BDA repair and reinforcement, future work should include adding main monitoring sites between 1N/1S and the confluence, at the confluence, on the unmonitored private property, the beaver complex, the bedrock notch, the late-season final-flow point, and an additional point on the alluvial fan upstream of site 4. These additional sites would help define surface flow patterns in relation to geology, vegetation regimes, and topography.

Bibliography

Bouwes, N., Weber, N., Jordan, C. E., Saunders, W. C., Tattam, I. A., Volk, C., & Pollock, M. M. (2016). Ecosystem experiment reveals benefits of natural and simulated beaver dams to a threatened population of steelhead (Oncorhynchus mykiss). *Scientific reports*, *6*, 28581.

Butler, D. R., & Malanson, G. P. (2005). The geomorphic influences of beaver dams and failures of beaver dams. *Geomorphology*, *71*(1-2), 48-60.

Castro, J. M. (Ed.). (2017). *The beaver restoration guidebook: Working with beaver to restore streams, wetlands, and floodplains*. US Fish and Wildlife Service.

Davee, R., Gosnell, H., & Charnley, S. (2019). Using beaver dam analogues for fish and wildlife recovery on public and private rangelands in eastern Oregon. *Res. Pap. PNW-RP-612. Portland, OR: US Department of Agriculture, Forest Service, Pacific Northwest Research Station. 29 p., 612*.

Duval, T. P., & Hill, A. R. (2006). Influence of stream bank seepage during low-flow conditions on riparian zone hydrology. Water Resources Research, 42(10).

Feiner, K., & Lowry, C. S. (2015). Simulating the effects of a beaver dam on regional groundwater flow through a wetland. *Journal of Hydrology: Regional Studies*, *4*, 675-685.

Gammons, C. H., Poulson, S. R., Pellicori, D. A., Reed, P. J., Roesler, A. J., & Petrescu, E. M. (2006). The hydrogen and oxygen isotopic composition of precipitation, evaporated mine water, and river water in Montana, USA. *Journal of Hydrology*, *328*(1-2), 319–330. https://doi.org/10.1016/j.jhydrol.2005.12.005

Goulden, M. L., & Bales, R. C. (2014). Mountain runoff vulnerability to increased evapotranspiration with vegetation expansion. Proceedings of the National Academy of Sciences, 111(39), 14071-14075.

Howard, R. J., & Larson, J. S. (1985). A stream habitat classification system for beaver. *The Journal of wildlife management*, 19-25.

Houghton, J. (2017). *Global Warming: The Complete Briefing* (5th ed.). Cambridge University Press.

Lautz, L., Kelleher, C., Vidon, P., Coffman, J., Riginos, C., & Copeland, H. (2019). Restoring stream ecosystem function with beaver dam analogues: Let's not make the same mistake twice. *Hydrological Processes*, *33*(1), 174-177.

Leflaive, X. (2012). OECD Environmental Outlook to 2050. *OECD Environmental Outlook.* https://doi.org/10.1787/9789264122246-en

Mitchell, C. C., & Niering, W. A. (1993). Vegetation change in a topogenic bog following beaver flooding. *Bulletin of the Torrey Botanical Club*, 136-147.

Nash, C. S., Grant, G. E., Charnley, S., Dunham, J. B., Gosnell, H., Hausner, M. B., ... & Taylor, J. D. (2021). Great expectations: Deconstructing the process pathways underlying beaver-related restoration. *BioScience*, *71*(3), 249-267.

Naiman, R. J., Melillo, J. M., & Hobbie, J. E. (1986). Ecosystem alteration of boreal forest streams by beaver (Castor canadensis). *Ecology*, *67*(5), 1254-1269.

Niezgoda, S. L. (2019, May). Design and Preliminary Evaluation of Beaver Dam Analogs to Reduce Downstream Sediment Loads: A Pilot Project in California Creek, Spokane, Washington, USA. In *World Environmental and Water Resources Congress 2019:*

Hydraulics, Waterways, and Water Distribution Systems Analysis (pp. 296-309). Reston, VA: American Society of Civil Engineers.

Nummi, P. (1989, January). Simulated effects of the beaver on vegetation, invertebrates and ducks. In *Annales Zoologici Fennici* (pp. 43-52). Finnish Zoological Publishing Board, formed by the Finnish Academy of Sciences, Societas Scientiarum Fennica, Societas pro Fauna et Flora Fennica and Societas Biologica Fennica Vanamo.

Nyssen, J., Pontzeele, J., & Billi, P. (2011). Effect of beaver dams on the hydrology of small mountain streams: example from the Chevral in the Ourthe Orientale basin, Ardennes, Belgium. Journal of hydrology, 402(1-2), 92-102.

Pearce, C., Vidon, P., Lautz, L., Kelleher, C., & Davis, J. (2021). Short-term impact of beaver dam analogues on streambank erosion and deposition in Semi-Arid landscapes of the Western USA. *River Research and Applications*, *37*(7), 1032-1037.

Pilliod, D. S., Rohde, A. T., Charnley, S., Davee, R. R., Dunham, J. B., Gosnell, H., ... & Nash, C. (2018). Survey of beaver-related restoration practices in rangeland streams of the western USA. *Environmental management*, *61*(1), 58-68.

Pollock, M. M., Beechie, T. J., Wheaton, J. M., Jordan, C. E., Bouwes, N., Weber, N., & Volk, C. (2014). Using beaver dams to restore incised stream ecosystems. *Bioscience*, *64*(4), 279-290.

Puttock, A., Graham, H. A., Cunliffe, A. M., Elliott, M., & Brazier, R. E. (2017). Eurasian beaver activity increases water storage, attenuates flow and mitigates diffuse pollution from intensively-managed grasslands. *Science of the total environment*, *576*, 430-443.

Scamardo, J., & Wohl, E. (2019). Assessing the potential for beaver restoration and likely environmental benefits. *Department of Geosciences, Colorado State University, Fort Collins, CO*.

Scamardo, J., & Wohl, E. (2020). Sediment storage and shallow groundwater response to beaver dam analogues in the Colorado Front Range, USA. *River Research and Applications*, *36*(3), 398-409.

Scarberry, K.C., Elliott, C.G., and Yakovlev, P.V. (2019). Geology of the Butte North 30' x 60' quadrangle, southwest Montana: Montana Bureau of Mines and Geology Open-File Report 715, 30 p., 1 sheet, scale 1:100,000.

Silverman, N. L., Allred, B. W., Donnelly, J. P., Chapman, T. B., Maestas, J. D., Wheaton, J. M., ... & Naugle, D. E. (2019). Low-tech riparian and wet meadow restoration increases vegetation productivity and resilience across semiarid rangelands. *Restoration Ecology*, *27*(2), 269-278.

Smith, J. M., & Mather, M. E. (2013). Beaver dams maintain fish biodiversity by increasing habitat heterogeneity throughout a low-gradient stream network. *Freshwater Biology*, *58*(7), 1523-1538.

Sophocleous, M. (2002). Interactions between groundwater and surface water: the state of the science. *Hydrogeology journal*, *10*(1), 52-67.

Wade, J., Lautz, L., Kelleher, C., Vidon, P., Davis, J., Beltran, J., & Pearce, C. (2020). Beaver dam analogues drive heterogeneous groundwater–surface water interactions. Hydrological Processes, 34(26), 5340-5353.

Water Science School. (2018, June 18). *Groundwater use in the United States*. Groundwater Use in the United States | U.S. Geological Survey. Retrieved January 21, 2022, from

https://www.usgs.gov/special-topics/water-science-school/science/groundwater-use-united-states

Weber, N., Bouwes, N., Pollock, M. M., Volk, C., Wheaton, J. M., Wathen, G., ... & Jordan, C. E. (2017). Alteration of stream temperature by natural and artificial beaver dams. *PloS one*, *12*(5), e0176313.

Wegener, P., Covino, T., & Wohl, E. (2017). Beaver-mediated lateral hydrologic connectivity, fluvial carbon and nutrient flux, and aquatic ecosystem metabolism. Water Resources Research, 53(6), 4606-4623.

Westbrook, C. J., Cooper, D. J., & Baker, B. W. (2006). Beaver dams and overbank floods influence groundwater–surface water interactions of a Rocky Mountain riparian area. *Water resources research*, *42*(6).

Westbrook, C. J., Cooper, D. J., & Butler, D. R. (2013). 12.20 Beaver Hydrology and Geomorphology.

Wickens, G. E. (1998). Arid and Semi-arid Environments of the World. In Ecophysiology of economic plants in arid and semi-arid lands (pp. 5-15). Springer, Berlin, Heidelberg.

Winter, R., 2014. A Practical Application of Salt Tracer Injections. Montana Technological University.

7. Appendix A: Site Data

A.1: Monitoring Site Locations

A.1.1: Main Monitoring Site Locations, Elevations

Site Number	Latitude (Decimal Degrees)	Longitude (Decimal Degrees)	Elevation (meters)
1N	46.174955	-112.692893	1779.23
1S	46.172777	-112.696616	1757.30
2	46.183545	-112.724227	1605.57
3	46.192639	-112.739193	1536.37
4	46.204939	-112.759425	1464.60

A.1.2: Late Season Monitoring Sub-Site Locations, Elevations

Reach	Sub- Site Number	Latitude (Decimal Degrees)	Longitude (Decimal Degrees)	Elevation (meters)
1 N	1	46.175414	-112.692687	1759
1 N	2	46.176108	-112.694442	1757
1 N	3	46.176240	-112.696771	1749
1 N	4	46.176737	-112.699078	1737
1 N	5	46.176922	-112.702974	1708
1 S	1	46.172411	-112.695791	1753
1 S	2	46.172812	-112.696934	1751
1 S	3	46.172508	-112.698748	1741
1 S	4	46.173439	-112.701777	1716
1 S	5	46.174201	-112.702692	1703
2	1	46.183545	-112.724227	1605
2	2	46.184602	-112.725092	1604
2	3	46.186889	-112.727000	1602
2	4	46.187358	-112.728314	1594
2	5	46.188622	-112.730633	1581
2	6	46.189272	-112.732175	1574
2	7	46.190386	-112.733567	1566
2	8	46.190963	-112.734894	1559
2	9	46.191422	-112.735527	1555
2	10	46.191329	-112.737699	1546
2	11	46.192716	-112.739093	1536

A.2: April to August Temporal Study

A.2.1: Site Summary Over Time

	4							
Date	Latitude	Longitude	Elevation (m)	Temperature (°C)	Conductivity (µs/cm)	Specific Conductivity (µs/cm)	Flow Rate (cfs)	Flow Rate (L/s)
04/03/21	46.2049386	-112.7594252	1464.597375	9.6	160.4	297.6	0.2591	7.3376
05/02/21	46.2049386	-112.7594252	1464.597375	8	144.7	295.3	1.9934	56.4471
5/9/21	46.2049386	-112.7594252	1464.597375	9.6	168.6	313.1	0.1290	3.6540
5/16/21	46.2049386	-112.7594252	1464.597375	19.9	226.1	266.9	0.2596	7.3503
5/23/21	46.2049386	-112.7594252	1464.597375	4.1	143.7	386.1	0.3142	8.8969
5/30/2021	46.2049386	-112.7594252	1464.597375					
6/9/2021	46.2049386	-112.7594252	1464.597375					
6/13/2021	46.2049386	-112.7594252	1464.597375					
6/20/2021	46.2049386	-112.7594252	1464.597375					
7/5/2021	46.2049386	-112.7594252	1464.597375					
7/18/2021	46.2049386	-112.7594252	1464.597375					
8/3/2021	46.2049386	-112.7594252	1464.597375					
8/22/2021	46.2049386	-112.7594252	1464.597375					
	3							
04/03/21	46.1926394	-112.7391929	1536.372396	6	142.6	331.5	0.8846	25.0487
05/02/21	46.1926394	-112.7391929	1536.372396	5.8	140.4	331.5	0.9181	25.9987
5/9/21	46.1926394	-112.7391929	1536.372396	6.2	153.5	351.6	0.2231	6.3165
5/16/21	46.1926394	-112.7391929	1536.372396	12.3	188.2	303.9	0.5985	16.9479
5/23/21	46.1926394	-112.7391929	1536.372396	3.3	141.6	407.1	0.6858	19.4192
5/30/2021	46.1926394	-112.7391929	1536.372396	14.9	197.4	283.2	0.5605	15.8730
6/9/2021	46.1926394	-112.7391929	1536.372396	12.2	200.1	324.3	0.1886	5.3404
6/13/2021	46.1926394	-112.7391929	1536.372396	12.9	193.9	306.5	0.3293	9.3244
6/20/2021	46.1926394	-112.7391929	1536.372396	12.6	203.9	324.6	0.2280	6.4575
7/5/2021	46.1926394	-112.7391929	1536.372396	12.9	200.5	314.8	0.0522	1.4794
7/18/2021	46.1926394	-112.7391929	1536.372396	12.9	212	332.3	0.0407	1.1529
8/3/2021	46.1926394	-112.7391929	1536.372396	17.3	232.3	302.6	0.0400	1.1325
8/22/2021	46.1926394	-112.7391929	1536.372396	14.6	228	330.7		
	2							
04/03/21	46.183545	-112.724227	1605.571066	2.6	117.7	356.7	0.8628	24.4307
05/02/21	46.183545	-112.724227	1605.571066	5	133	332.2	1.6593	46.9852
5/9/21	46.183545	-112.724227	1605.571066	4.3	140.5	170.3	0.2765	7.8293
5/16/21	46.183545	-112.724227	1605.571066	10.3	172.6	309.2	0.1760	4.9842
5/23/21	46.183545	-112.724227	1605.571066	2.6	134.7	411	0.5214	14.7631
5/30/2021	46.183545	-112.724227	1605.571066	10.4	174.6	310	1.1803	33.4225
6/9/2021	46.183545	-112.724227	1605.571066	10.8	185	322.2	0.2757	7.8071
6/13/2021	46.183545	-112.724227	1605.571066	12.3	193.8	312.6	0.4761	13.4807
6/20/2021	46.183545	-112.724227	1605.571066	10.7	189.8	332	0.2419	6.8499
7/5/2021	46.183545	-112.724227	1605.571066	12	206.8	339.5	0.0634	1.7957
7/18/2021	46.183545	-112.724227	1605.571066	14.7	100	145.7	0.0178	0.5046
8/3/2021	46.183545	-112.724227	1605.571066					
8/22/2021	46.183545	-112.724227	1605.571066					
	2							
04/03/21	46.183545	-112.724227	1605.571066	2.6	117.7	356.7	0.8628	24.4307
05/02/21	46.183545	-112.724227	1605.571066	5	133	332.2	1.6593	46.9852
5/9/21	46.183545	-112.724227	1605.571066	4.3	140.5	170.3	0.2765	7.8293
5/16/21	46.183545	-112.724227	1605.571066	10.3	172.6	309.2	0.1760	4.9842
5/23/21	46.183545	-112.724227	1605.571066	2.6	134.7	411	0.5214	14.7631
5/30/2021	46.183545	-112.724227	1605.571066	10.4	174.6	310	1.1803	33.4225
6/9/2021	46.183545	-112.724227	1605.571066	10.8	185	322.2	0.2757	7.8071
6/13/2021	46.183545	-112.724227	1605.571066	12.3	193.8	312.6	0.4761	13.4807
6/20/2021	46.183545	-112.724227	1605.571066	10.7	189.8	332	0.2419	6.8499
7/5/2021	46.183545	-112.724227	1605.571066	12	206.8	339.5	0.0634	1.7957
7/18/2021	46.183545	-112.724227	1605.571066	14.7	100	145.7	0.0178	0.5046
8/3/2021	46.183545	-112.724227	1605.571066					
8/22/2021	46.183545	-112.724227	1605.571066					
	1S							
04/03/21	46.172777	-112.696616	1757.295257					
05/02/21	46.172777	-112.696616	1757.295257	3.6	120.7	337.9	0.3220	9.1167
5/9/21	46.172777	-112.696616	1757.295257	2.7	127.1	389	0.1386	3.9260
5/16/21	46.172777	-112.696616	1757.295257	9.4	141.5	265.6	0.2403	6.8032
5/23/21	46.172777	-112.696616	1757.295257					
5/30/2021	46.172777	-112.696616	1757.295257	10.6	167.2	293.6	0.2839	8.0401
6/9/2021	46.172777	-112.696616	1757.295257					
6/13/2021	46.172777	-112.696616	1757.295257	14.7	193.9	280.5	0.1851	5.2405
6/20/2021	46.172777	-112.696616	1757.295257	10.6	181	317.9	0.1697	4.8065
7/5/2021	46.172777	-112.696616	1757.295257	13.9	134.3	199.7	0.3725	10.5474
7/18/2021	46.172777	-112.696616	1757.295257	13.9	209.6	314.7	0.0598	1.6920
8/3/2021	46.172777	-112.696616	1757.295257	14.9	241	298.4	0.0712	2.0175
8/22/2021	46.172777	-112.696616	1757.295257	11.5	210.6	353.8	0.1758	4.9767
	1N							
04/03/21	46.174955	-112.692893	1779.226768					
05/02/21	46.174955	-112.692893	1779.226768	8	146.7	300	0.3773	10.6843
5/9/21	46.174955	-112.692893	1779.226768	3.1	120.6	352	0.1386	3.9260
5/16/21	46.174955	-112.692893	1779.226768	10.4	122.8	218.8	0.3025	8.5653
5/23/21	46.174955	-112.692893	1779.226768					
5/30/2021	46.174955	-112.692893	1779.226768	11	154.8	267.6	0.4119	11.6627
6/9/2021	46.174955	-112.692893	1779.226768					
6/13/2021	46.174955	-112.692893	1779.226768	15	185.9	266	0.1702	4.8205
6/20/2021	46.174955	-112.692893	1779.226768	10.6	172.9	304.3	0.1713	4.8520
7/5/2021	46.174955	-112.692893	1779.226768	14.4	174.7	256.8	0.0651	1.8437
7/18/2021	46.174955	-112.692893	1779.226768	15.6	211.9	295.5	0.0503	1.4252
8/3/2021	46.174955	-112.692893	1779.226768	16.4	187.2	239.1	0.0815	2.3073
8/22/2021	46.174955	-112.692893	1779.226768	12.5	191.1	305.1	0.1135	3.2134

*** ~ indicates dry conditions, dates on which no date was collected are left blank***

A.2.2: Reach Water Balance

Reach	Date	Upstream Discharge (cfs)	Downstream Discharge (cfs)	Groundwater Discharge (cfs)	Groundwater Discharge (L/s)
1	04/03/21	0.00	0.86	0.86	24.43
	05/02/21	0.70	1.66	0.96	27.18
	5/9/21	0.28	0.28	0.00	0.00
	5/16/21	0.54	0.18	-0.37	-10.38
	5/23/21	0.00	0.52	0.52	14.76
	5/30/2021	0.70	1.18	0.48	13.72
	6/9/2021	0.00	0.28	0.28	7.81
	6/13/2021	0.36	0.48	0.12	3.42
	6/20/2021	0.34	0.24	-0.10	-2.81
	7/5/2021	0.44	0.06	-0.37	-10.60
	7/18/2021	0.11	0.02	-0.09	-2.61
	8/3/2021	0.15	0.00	-0.15	-4.32
	8/22/2021	0.29	0.00	-0.29	-8.19
2	04/03/21	0.86	0.88	0.02	0.62
	05/02/21	1.66	0.92	-0.74	-20.99
	5/9/21	0.28	0.22	-0.05	-1.51
	5/16/21	0.18	0.60	0.42	11.96
	5/23/21	0.52	0.69	0.16	4.66
	5/30/2021	1.18	0.56	-0.62	-17.55
	6/9/2021	0.28	0.19	-0.09	-2.47
	6/13/2021	0.48	0.33	-0.15	-4.16
	6/20/2021	0.24	0.23	-0.01	-0.39
	7/5/2021	0.06	0.05	-0.01	-0.32
	7/18/2021	0.02	0.04	0.02	0.65
	8/3/2021	0.00	0.04	0.04	1.13
	8/22/2021	0.00	0.00	0.00	0.00
3	04/03/21	0.88	0.26	-0.63	-17.71
	05/02/21	0.92	0.00	-0.92	-26.00
	5/9/21	0.22	0.13	-0.09	-2.66
	5/16/21	0.60	0.26	-0.34	-9.60
	5/23/21	0.69	0.31	-0.37	-10.52
	5/30/2021	0.56	0.00	-0.56	-15.87
	6/9/2021	0.19	0.00	-0.19	-5.34
	6/13/2021	0.33	0.00	-0.33	-9.32
	6/20/2021	0.23	0.00	-0.23	-6.46
	7/5/2021	0.05	0.00	-0.05	-1.48
	7/18/2021	0.04	0.00	-0.04	-1.15
	8/3/2021	0.04	0.00	-0.04	-1.13
	8/22/2021	0	0	0.00	0.00

*** “0.00” indicates either no data collected or dry conditions***

A.2.3: Load Balance

Reach	Date	Upstream SC (uS/cm)	Downstream SC (uS/cm)	Upstream Discharge (cfs)	Downstream Discharge (cfs)	Groundwater Discharge (cfs)	Groundwater SC (uS/cm)
1	04/03/21		356.70	0.00	0.86	0.86	356.70
	05/02/21	318.95	332.20	0.70	1.66	0.96	341.85
	5/9/21	370.50	170.30	0.28	0.28	0.00	69390.32
	5/16/21	242.20	309.20	0.54	0.18	-0.37	210.04
	5/23/21		411.00	0.00	0.52	0.52	411.00
	5/30/2021	280.60	310.00	0.70	1.18	0.48	352.22
	6/9/2021		322.20	0.00	0.28	0.28	322.20
	6/13/2021	273.25	312.60	0.36	0.48	0.12	428.37
	6/20/2021	311.10	332.00	0.34	0.24	-0.10	260.13
	7/5/2021	228.25	339.50	0.44	0.06	-0.37	209.40
	7/18/2021	305.10	145.70	0.11	0.02	-0.09	335.89
	8/3/2021	268.75		0.15	0.00	-0.15	268.75
	8/22/2021	329.45		0.29	0.00	-0.29	329.45
2	04/03/21	356.70	331.50	0.86	0.88	0.02	664.67
	05/02/21	332.20	331.50	1.66	0.92	-0.74	333.07
	5/9/21	170.30	351.60	0.28	0.22	-0.05	586.70
	5/16/21	309.20	303.90	0.18	0.60	0.42	301.69
	5/23/21	411.00	407.10	0.52	0.69	0.16	394.73
	5/30/2021	310.00	283.20	1.18	0.56	-0.62	334.24
	6/9/2021	322.20	324.30	0.28	0.19	-0.09	317.65
	6/13/2021	312.60	306.50	0.48	0.33	-0.15	326.29
	6/20/2021	332.00	324.60	0.24	0.23	-0.01	453.78
	7/5/2021	339.50	314.80	0.06	0.05	-0.01	455.01
	7/18/2021	145.70	332.30	0.02	0.04	0.02	477.56
	8/3/2021		302.60	0.00	0.04	0.04	302.60
	8/22/2021			0.00	0.00	0.00	
3	04/03/21	331.50	297.60	0.88	0.26	-0.63	345.54
	05/02/21	331.50	295.30	0.92		-0.92	331.50
	5/9/21	351.60	313.10	0.22	0.13	-0.09	404.44
	5/16/21	303.90	266.90	0.60	0.26	-0.34	332.24
	5/23/21	407.10	386.10	0.69	0.31	-0.37	424.86
	5/30/2021	283.20		0.56	0.00	-0.56	283.20
	6/9/2021	324.30		0.19	0.00	-0.19	324.30
	6/13/2021	306.50		0.33	0.00	-0.33	306.50
	6/20/2021	324.60		0.23	0.00	-0.23	324.60
	7/5/2021	314.80		0.05	0.00	-0.05	314.80
	7/18/2021	332.30		0.04	0.00	-0.04	332.30
	8/3/2021	302.60		0.04	0.00	-0.04	302.60
	8/22/2021			0.00	0.00	0.00	

Blank cells indicate no data/dry conditions, red cells indicate erroneous date points

A.2.4: Two-Component Mixing

Site	Date	River SC (uS/cm)	Overland SC (uS/cm)	Groundwater SC (uS/cm)	Overland Fraction	Groundwater Fraction	Stream Discharge (cfs)	Overland Discharge (cfs)	Groundwater Discharge (cfs)	Stream Discharge (L/s)	Overland Discharge (L/s)	Groundwater Discharge (L/s)
4	04/03/21	297.6	120	335.57	0.18	0.82	0.26	0.05	0.21	7.34	1.29	6.05
	05/02/21	295.3	120	335.57	0.19	0.81		0.00	0.00	0.00	0.00	0.00
	5/9/21	313.1	120	335.57	0.10	0.90	0.13	0.01	0.12	3.65	0.38	3.27
	5/16/21	266.9	120	335.57	0.32	0.68	0.26	0.08	0.18	7.35	2.34	5.01
	5/23/21	386.1	120	335.57	-0.23	1.23	0.31	-0.07	0.39	8.90	-2.09	10.98
	5/30/2021											
	6/9/2021											
	6/13/2021											
	6/20/2021											
	7/5/2021											
	7/18/2021											
	8/3/2021											
	8/22/2021											
3	04/03/21	331.5	120	373.95	0.17	0.83	0.88	0.15	0.74	25.05	4.19	20.86
	05/02/21	331.5	120	373.95	0.17	0.83	0.92	0.15	0.76	26.00	4.35	21.65
	5/9/21	351.6	120	373.95	0.09	0.91	0.22	0.02	0.20	6.32	0.56	5.76
	5/16/21	303.9	120	373.95	0.28	0.72	0.60	0.17	0.43	16.95	4.68	12.27
	5/23/21	407.1	120	373.95	-0.13	1.13	0.69	-0.09	0.78	19.42	-2.53	21.95
	5/30/2021	283.2	120	373.95	0.36	0.64	0.56	0.20	0.36	15.87	5.67	10.20
	6/9/2021	324.3	120	373.95	0.20	0.80	0.19	0.04	0.15	5.34	1.04	4.30
	6/13/2021	306.5	120	373.95	0.27	0.73	0.33	0.09	0.24	9.32	2.48	6.85
	6/20/2021	324.6	120	373.95	0.19	0.81	0.23	0.04	0.18	6.46	1.25	5.20
	7/5/2021	314.8	120	373.95	0.23	0.77	0.05	0.01	0.04	1.48	0.34	1.13
	7/18/2021	332.3	120	373.95	0.16	0.84	0.04	0.01	0.03	1.15	0.19	0.96
	8/3/2021	302.6	120	373.95	0.28	0.72	0.04	0.01	0.03	1.13	0.32	0.81
	8/22/2021											
2	04/03/21	356.7	120	365.58	0.04	0.96	0.86	0.03	0.83	24.43	0.88	23.55
	05/02/21	332.2	120	365.58	0.14	0.86	1.66	0.23	1.43	46.99	6.39	40.60
	5/9/21	170.3	120	365.58	0.80	0.20	0.28	0.22	0.06	7.83	6.23	1.60
	5/16/21	309.2	120	365.58	0.23	0.77	0.18	0.04	0.14	4.98	1.14	3.84
	5/23/21	411	120	365.58	-0.18	1.18	0.52	-0.10	0.62	14.76	-2.73	17.49
	5/30/2021	310	120	365.58	0.23	0.77	1.18	0.27	0.91	33.42	7.56	25.86
	6/9/2021	322.2	120	365.58	0.18	0.82	0.28	0.05	0.23	7.81	1.38	6.43
	6/13/2021	312.6	120	365.58	0.22	0.78	0.48	0.10	0.37	13.48	2.91	10.57
	6/20/2021	332	120	365.58	0.14	0.86	0.24	0.03	0.21	6.85	0.94	5.91
	7/5/2021	339.5	120	365.58	0.11	0.89	0.06	0.01	0.06	1.80	0.19	1.60
	7/18/2021	145.7	120	365.58	0.90	0.10	0.02	0.02	0.00	0.50	0.45	0.05
	8/3/2021											
	8/22/2021											
1S	04/03/21											
	05/02/21	337.9	120	318.83	-0.10	1.10	0.32	-0.03	0.35	9.12	-0.87	9.99
	5/9/21	389	120	318.83	-0.35	1.35	0.14	-0.05	0.19	3.93	-1.39	5.31
	5/16/21	265.6	120	318.83	0.27	0.73	0.24	0.06	0.18	6.80	1.82	4.98
	5/23/21		120	318.83								
	5/30/2021	293.6	120	318.83	0.13	0.87	0.28	0.04	0.25	8.04	1.02	7.02
	6/9/2021		120	318.83				0	0	0	0	0
	6/13/2021	280.5	120	318.83	0.19	0.81	0.19	0.04	0.15	5.24	1.01	4.23
	6/20/2021	317.9	120	318.83	0.00	1.00	0.17	0.00	0.17	4.81	0.02	4.78
	7/5/2021	199.7	120	318.83	0.60	0.40	0.37	0.22	0.15	10.55	6.32	4.23
	7/18/2021	314.7	120	318.83	0.02	0.98	0.06	0.00	0.06	1.69	0.04	1.66
	8/3/2021	298.4	120	318.83	0.10	0.90	0.07	0.01	0.06	2.02	0.21	1.81
	8/22/2021	353.8	120	318.83	-0.18	1.18	0.18	-0.03	0.21	4.98	-0.88	5.85
1N	04/03/21											
	05/02/21	300	120	318.83	0.09	0.91	0.38	0.04	0.34	10.68	1.01	9.67
	5/9/21	352	120	318.83	-0.17	1.17	0.14	-0.02	0.16	3.93	-0.65	4.58
	5/16/21	218.8	120	318.83	0.50	0.50	0.30	0.15	0.15	8.57	4.31	4.26
	5/23/21											
	5/30/2021	267.6	120	318.83	0.26	0.74	0.41	0.11	0.31	11.66	3.01	8.66
	6/9/2021											
	6/13/2021	266	120	318.83	0.27	0.73	0.17	0.05	0.13	4.82	1.28	3.54
	6/20/2021	304.3	120	318.83	0.07	0.93	0.17	0.01	0.16	4.85	0.35	4.50
	7/5/2021	256.8	120	318.83	0.31	0.69	0.07	0.02	0.04	1.84	0.58	1.27
	7/18/2021	295.5	120	318.83	0.12	0.88	0.05	0.01	0.04	1.43	0.17	1.26
	8/3/2021	239.1	120	318.83	0.40	0.60	0.08	0.03	0.05	2.31	0.93	1.38
	8/22/2021	305.1	120	318.83	0.07	0.93	0.11	0.01	0.11	3.21	0.22	2.99
1 Combined	04/03/21											
	05/02/21						0.70	0.00	0.69	19.80	0.14	19.66
	5/9/21						0.28	-0.07	0.35	7.85	-2.04	9.89
	5/16/21						0.54	0.22	0.33	15.37	6.13	9.24
	5/23/21											
	5/30/2021						0.70	0.14	0.55	19.70	4.03	15.68
	6/9/2021											
	6/13/2021						0.36	0.08	0.27	10.06	2.29	7.77
	6/20/2021						0.34	0.01	0.33	9.66	0.38	9.28
	7/5/2021						0.44	0.24	0.19	12.39	6.89	5.50
	7/18/2021						0.11	0.01	0.10	3.12	0.20	2.91
	8/3/2021						0.15	0.04	0.11	4.32	1.13	3.19
	8/22/2021						0.29	-0.02	0.31	8.19	-0.65	8.84

A.2.5: Isotopes

	4		3		2		1S		1N	
Date	**$\delta^{18}O$**	**$\delta^{2}H$**	**$\delta^{18}O$**	**$\delta^{2}H$**	**$\delta^{18}O$**	**$\delta^{2}H$**	**$\delta^{18}O$**	**$\delta^{2}H$**	**$\delta^{18}O$**	**$\delta^{2}H$**
4/3/2021	-17.288	-135.649	-17.308	-136.573	-17.526	-136.190				
5/2/2021	-16.950	-133.432	-16.693	-133.952	-15.531	-134.073	-13.290	-132.782	-17.172	-136.268
5/9/2021	-17.073	-133.625	-13.679	-134.370	-17.163	-134.408	-15.295	-133.807	-17.219	-135.307
5/16/2021	-17.045	-133.583	-17.076	-134.080	-17.133	-133.988	-15.963	-130.893	-17.153	-135.061
5/23/2021	-17.119	-134.498	-17.151	-134.317	-17.229	-133.673				
5/30/2021										
6/9/2021			-14.018	-133.342	-16.814	-133.009				
6/13/2021			-17.001	-133.958	-16.556	-130.295	-16.262	-131.229	-13.893	-134.814
6/20/2021			-17.093	-134.550	-13.551	-134.221	-13.471	-134.509	-17.048	-134.945
7/5/2021			-17.215	-134.943	-16.997	-133.768	-16.721	-134.450	-17.448	-135.013
7/18/2021			-17.072	-134.094	-16.849	-132.902	-17.211	-134.064	-17.032	-134.546
8/3/2021			-17.096	-133.791	-16.997	-133.891	-16.889	-133.636	-17.284	-134.500
8/22/2021			-16.925	-134.004			-16.534	-130.635	-17.246	-134.441

A.3 Late Season High-Definition Spatial Study

A.3.1: Sub-Site Summary

Reach	Site Number	Latitude	Longitude	Temperature (°C)	Conductivity (µs/cm)	Specific Conductivity (µs/cm)	Flow Rate (L/s)	Flow Rate (cfs)
1N	1	46.175414	-112.692687	16.4	187.2	239.10	2.298321	0.081164
1N	2	46.176108	-112.694442	14.9	197.4	284.00	2.181080	0.077024
1N	3	46.176240	-112.696771	12.8	205.3	323.80	1.003968	0.035455
1N	4	46.176737	-112.699078	12.7	199.3	315.50	1.181293	0.041717
1N	5	46.176922	-112.702974	12.7	199.3	315.50	1.231392	0.043486
1S	1	46.172411	-112.695791	14.9	241.0	298.40	2.017524	0.071248
1S	2	46.172812	-112.696934			303.10	1.758882	0.062114
1S	3	46.172508	-112.698748	14.0	227.3	287.60	2.118128	0.074801
1S	4	46.173439	-112.701777	14.1	240.8	304.40	2.371178	0.083737
1S	5	46.174201	-112.702692	13.8	238.2	303.30	1.717989	0.060670
1	1						4.315845	0.152413
1	2						3.939962	0.139138
1	3						3.122097	0.110256
1	4						3.552470	0.125454
1	5						2.949381	0.104156
2	1	46.183526	-112.724352				0.000000	0.000000
2	2	46.184602	-112.725092	18.5	248.5	309.2	2.527115	0.089244
2	3	46.186889	-112.727000				0.000000	0.000000
2	4	46.187358	-112.728314				0.000000	0.000000
2	6	46.189272	-112.732175	11.2	105	179.3	2.394246	0.084552
2	8	46.190963	-112.734894	18	240.4	305.1	1.233246	0.043552
2	9	46.191422	-112.735527	18.3	249.1	312.3	5.528784	0.195247
2	10	46.191329	-112.737699	17.5	244.6	315.8	1.116328	0.039423
2	11	46.192716	-112.739093	17.3	232.3	302.6	1.221642	0.043142

*** Blank cells indicate no data, “0” in Flow Rate columns indicate dry conditions. Reach 1 is the combined reach of 1S and 1N***

A.3.2: Surface Balance

Reach	Sub Reach	Upstream Discharge (cfs)	Downstream Discharge (cfs)	Groundwater Discharge (cfs)	Groundwater Discharge (L/s)
1	1	0.152	0.139	-0.013	-0.376
	2	0.139	0.110	-0.029	-0.818
	3	0.110	0.125	0.015	0.430
	4	0.125	0.104	-0.021	-0.603
1N	1	0.081	0.077	-0.004	-0.117
	2	0.077	0.035	-0.042	-1.177
	3	0.035	0.042	0.006	0.177
	4	0.042	0.043	0.002	0.050
1S	1	0.071	0.062	-0.009	-0.259
	2	0.062	0.075	0.013	0.359
	3	0.075	0.084	0.009	0.253
	4	0.084	0.061	-0.023	-0.653
2	1	0.000	0.089	0.089	2.527
	2	0.089	0.000	-0.089	-2.527
	3	0.000	0.000	0.000	0.000
	4	0.000	0.000	0.000	0.000
	5	0.000	0.085	0.085	2.394
	6	0.085	0.044	-0.041	-1.161
	8	0.044	0.195	0.152	4.296
	9	0.195	0.039	-0.156	-4.412
	10	0.039	0.043	0.004	0.105

A.3.3: Load Balance

Reach	Sub reach	Upstream SC (uS/cm)	Downstream SC (uS/cm)	Upstream Discharge (cfs)	Downstream Discharge (cfs)	Groundwater Discharge (cfs)	Groundwater SC (uS/cm)
1	1			0.152	0.139	-0.013	
	2			0.139	0.110	-0.029	
	3			0.110	0.125	0.015	
	4			0.125	0.104	-0.021	
1N	1	239.10	284.00	0.081	0.077	-0.004	596.190
	2	284.00	323.80	0.077	0.035	-0.042	250.054
	3	323.80	315.50	0.035	0.042	0.006	268.507
	4	315.50	315.50	0.042	0.043	0.002	315.500
1S	1	298.40	303.10	0.071	0.062	-0.009	266.438
	2	303.10	287.60	0.062	0.075	0.013	211.712
	3	287.60	304.40	0.075	0.084	0.009	445.023
	4	304.40	303.30	0.084	0.061	-0.023	307.293
2	1			0.000	0.089	0.089	
	2	309.20	179.30	0.089	0.000	-0.089	309.200
	3			0.000	0.000	0.000	
	4			0.000	0.000	0.000	
	5			0.000	0.085	0.085	
	6	179.30	305.10	0.085	0.044	-0.041	45.672
	8	305.10	312.30	0.044	0.195	0.152	314.367
	9	312.30	315.80	0.195	0.039	-0.156	311.415
	10	315.80	302.60	0.039	0.043	0.004	162.681

Empty cells indicate no data or dry conditions. Red cells indicate erroneous data points

A.3.4: Soil Moisture Content

Reach	Sub Site	Sample Location	Depth Interval (in)	Tin Weight	Wet Weight (+Tin) (g)	Wet Weight (g)	Dry Weight (+Tin) (g)	Dry Weight (g)	Moisture content (g)	Percent Moisture (%)
2	1	46.183526 -112.724352	0 to 7	11.22	25.27	14.05	24.77	13.55	0.50	3.54
	1	46.183526 -112.724352	7 to 13	11.23	30.61	19.37	30.20	18.97	0.41	2.10
	2	46.184602 -112.725092	0 to 4	11.29	31.13	19.83	30.70	19.41	0.43	2.14
	2	46.184602 -112.725092	4 to 14	11.24	48.09	36.85	43.42	32.18	4.67	12.68
	2	46.184602 -112.725092	14 to 26	11.17	50.44	39.27	43.41	32.24	7.03	17.91
	5 to 6	46.189153 -112.731615	0 to 7	11.26	44.41	33.15	44.28	33.02	0.13	0.39
	5 to 6	46.189153 -112.731615	7 to 10	11.09	25.69	14.60	25.59	14.49	0.10	0.71
	5 to 6	46.189153 -112.731615	10 to 22	11.22	51.95	40.73	38.48	27.26	13.47	33.08
	5 to 6	46.189153 -112.731615	22 to 36	11.15	58.62	47.47	48.41	37.26	10.21	21.51
	5 to 6	46.189153 -112.731615	36 to 48	11.19	47.42	36.23	39.30	28.11	8.12	22.41
	5 to 6	46.189153 -112.731615	48 to 58	15.75	72.29	56.54	62.24	46.49	10.05	17.77
	8	46.190963 -112.734894	0 to 8	15.68	52.88	37.20	49.82	34.14	3.06	8.23
	9	46.191422 -112.735527	0 to 5	20.33	48.65	28.32	43.57	23.24	5.08	17.94
	9	46.191422 -112.735527	5 to 6.5	13.88	28.44	14.56	28.35	14.47	0.09	0.63
	9	46.191422 -112.735527	6.5 to 12	15.70	51.60	35.90	51.07	35.37	0.53	1.48
	10	46.191329 -112.737699	0 to 12	15.83	54.99	39.16	51.59	35.76	3.40	8.68
	10	46.191329 -112.737699	12 to 24	21.60	74.50	52.91	67.35	45.76	7.15	13.51
	10	46.191329 -112.737699	24 to 30	21.56	72.26	50.70	71.37	49.81	0.89	1.76
	10	46.191329 -112.737699	30 to 35	21.55	57.77	36.22	57.20	35.65	0.57	1.57

A.3.5: Principal Clays

		Sample Location			Principal Clay Minerals		
Reach	Sub Site	Latitude	Longitude	Depth (in)	Mineral 1	Mineral 2	Mineral 3
2	1	46.18353	-112.724352	0-7	Iron Saponite	Dolomite	Halloysite
	1	46.18353	-112.724352	7 to 13	Iron Saponite	Halloysite	
	2	46.1846	-112.725092	0 to 4	Iron Saponite	Axinite	Muscovite
	2	46.1846	-112.725092	4 to 14	Iron Saponite	Muscovite	
	2	46.1846	-112.725092	14 to 26	Iron Saponite	Muscovite	
	5 & 6	46.18915	-112.731615	0 to 7	Iron Saponite	Muscovite	Axinite
	5 & 6	46.18915	-112.731615	7 to 10	Iron Saponite	Muscovite	Axinite
	5 & 6	46.18915	-112.731615	10 to 22	Iron Saponite	Vermiculite	
	5 & 6	46.18915	-112.731615	22 to 36	Montmorillonite	Phlogopite	
	5 & 6	46.18915	-112.731615	36 to 48	Montmorillonite		
	5 & 6	46.18915	-112.731615	48 to 58	Montmorillonite	Phlogopite	Halloysite
	8	46.19096	-112.734894	0 to 8	Iron Saponite	Halloysite	
	9	46.19142	-112.735527	0 to 5	Iron Saponite		
	9	46.19142	-112.735527	5 to 6.5	Iron Saponite	Muscovite	
	9	46.19142	-112.735527	6.5 to 12	Iron Saponite	Muscovite	
	10	46.19133	-112.737699	0 to 12	Montmorillonite		
	10	46.19133	-112.737699	12 to 24	Montmorillonite		
	10	46.19133	-112.737699	24 to 30	Montmorillonite	Vermiculite	
	10	46.19133	-112.737699	30 to 35	Montmorillonite	Vermiculite	

8. Appendix B: Site Images and Features of Note

B.1: Monitoring Sites

B.1.1: Perkins Gulch Monitoring Site 4

B.1.2: Perkins Gulch Monitoring Site 3

B.1.3: Perkins Gulch Monitoring Site 2

B.1.4: Perkins Gulch Monitoring Site 1S

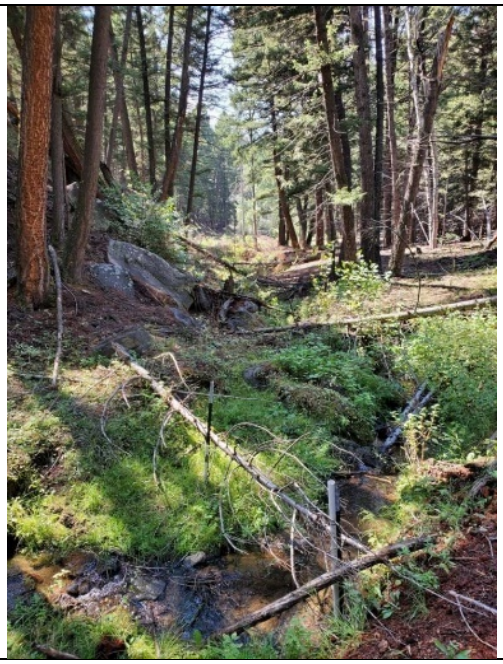

B.1.5: Perkins Gulch Monitoring Site 1N

B.1.6: Bedrock Notch and Sweetwater Creek (Tscs) Outcrop

B.1.7: Abandoned Beaver Complex

B.1.8: Meadow Wetland at Perkins Gulch Monitoring Site 2

B.2: BDA Structures in Reach 2

B.2.1: Partially Blown-Out BDA and Aggraded Stream at Site 3

B.2.2: Blown-Out BDA at Site 2

B.2.3: Intact BDA and Pooling Stream at Site 2

B.2.4: Blown-Out BDA and Meandering Stream at Site 2

B.2.5: Blown-Out BDA, Aggrading Point Bar and Cutbank at Site 2

B.2.6: Blown-Out BDA with New Channelization and Increased Vegetation at Site 2